Numerical Model of Air Blast & Weapon Effects

Jinpeng Zhai

December 28, 2022

Abstract

TBD

Contents

1 Preliminary Note

Two DOS programs, BLAST and WE (for Weapon Effects) produced by Horizons Technology for the Defense Nuclear Agency, dating to 1984, has been acquired by the present author through online, public sources.

It is believed that these programs were considered "verified" by the then US Defense Nuclear Agency, and much of the result from this program corroborates that found in other, prominent sources.

The programs built in help pages self-documented the models underlying many aspects of nuclear weapon effects, coming to results that is otherwise only available from manual consultation and interpolation of many graphs and tables.

These models have been reproduced in a more accessible format in one other publication, as far as this author is aware. However, there are several mistakes and ambiguities from the original documentation that remains unresolved. This work attempts to reproduce and validate the models both with the original software's outputs and other sources publicly available.

The $\mathtt{function} < \mathtt{parameter} >$ notation is used to indicate call to a function, and either $\cdot$ or $\times$ are used for explicit multiplication. Minimal use of implicit multiplication allows disambiguation of multiple-letter variable. , is used for thousand separator and . for decimal point.

2 Airburst models

The blast models were able to be exactly reproduced for all parameters except for those associated with impulse.

The procedure documented in this paragraph results in a lower dynamic pressure, a shorter overpressure & dynamic pressure positive phase duration,, and finally less impulse, as compared to published data. This is likely attributed to the problematic $\mathtt{dp}_{\mathtt{unmod}}$ formulation. It is for this reason that a fall-back procedure has been detailed in the appendix, taken from one of the source cited below.

`This program calculates the peak overpressure and the peak dynamic pressure at the surface of the earth as a function of height of burst, ground range, and weapon yield. The surface is treated as "near-ideal," with no account of mechanical effects of the surface (for example, buildings and terrain with appreciably varying slope affect the shock front, and deformable material will absorb some of the blast energy). Also neglected are thermal effects due to absorption of heat by the surface (to form a layer of heated air that distorts the blast wave) and involvement of surface material ("dust") with the flow. Hence, the calculations apply to relatively flat, rigid, clean and thermally reflective surfaces.`

`The incident blast wave is reflected by the surface, and beyond a certain ground range (called the Mach stem formation range) this reflected wave merges with the incident wave to produce a stronger shock in what is called the Mach reflection region. The region inside the Mach stem formation range is known as the regular reflection region. For peak overpressure below about 350 kPa this merging has a marked effect: the highest peak overpressure at a given yield and ground range is produced for a height of burst somewhat above zero.`

`The air-burst peak overpressure fit is based in part on the DNA 1- kiloton free-air Standard. The results at all ground ranges from a surface burst are consistent`

with this model (using twice-yield scaling); the results for the point on the ground directly below the burst are also consistent (using the free-air normal reflection factor), for all heights of burst within the model limits. Other points on the overpressure curves are from curve fits based on data from Carpenter (see SOURCES OF DATA below).

The air-burst peak dynamic pressure of a reflected shock in the Mach reflection region is calculated from Rankine-Hugoniot relations applied to the merged shock front. In the regular reflection region, the shape of the dynamic-pressure height-of-burst curves (contours in height-of-burst, ground-range space) is determined from theory, but approximated by a simpler function in this program. The two regions, regular and Mach, have been merged by a switching function that is centered near the onset of Mach stem formation.

A calculation is provided to determine the Mach stem formation range (as a function of height of burst), and the height of the triple point (the point at which the Mach stem, incident shock front, and reflected shock meet) for distances larger than the Mach stem formation range.

The other air-burst calculations this program provides involve the dependence of pressure (either overpressure or dynamic pressure) on time. These time-dependent calculations (also known as wave-form calculations) are:

- Partial and total impulses
- Time-dependent pressures
- Positive phase durations

The impulse calculations numerically integrate the time-dependent pressure functions with respect to time. A total impulse is integrated from the time of the blast wave arrival until the time-dependent pressure reaches zero (that is, for the entire duration of the positive phase). A partial impulse is a similar integration of pressure versus time, but to a final time less than the positive phase duration.

The classical shape of the waveform is a sharp peak at the time the blast waves arrives, followed by a quick decay to zero. However, it has been found that in certain cases the highest pressures do not occur at the time of arrival of the shock front. In the transition region from regular to Mach reflection, for peak overpressures larger than roughly 700 kPa, the overpressure waveform can have two peaks, and the second maximum may be larger than the first. Building upon empirical waveform experiments by Carpenter and on calculations, Speicher and Brode have developed a model of the double-peaked overpressure waveform.

The dynamic pressure waveform model is approximated by using a variation on the overpressure waveform as a starting point. It is known that the resulting dynamic pressure waveforms are not always realistic, since investigations have shown that a dynamic pressure maximum can occur between the two overpressure peaks. Nevertheless, it is a reasonable approximation in light of scarce dynamic pressure data. In the fully- developed Mach region, where waveforms are similar to the classical wave- form model, the dynamic pressure waveforms are good.

The waveform calculation models used by this program are derived from work done by Speicher and Brode (see SOURCES OF DATA below) with a few modifications. Simpler fits to Carpenter's peak overpressure data have been substituted for those of Speicher and Brode, and used in the peak dynamic pressure models. A slightly

different time-of-arrival function has also been used. Other changes have been made to the Speicher and Brode waveform models to bring some of the total impulse calculations into closer agreement with the REFLECT-4 code work done by Smiley, Ruetenik and Tomayko. For the overpressure waveform model a slight modification of the positive phase duration was made. This modification has not degraded the overpressure versus time fit; in fact, comparisons with REFLECT-4 waveforms showed some improvements in the overpressure model.

More extensive changes have been made to the dynamic pressure model. The positive phase duration was replaced with a new fit based on the REFLECT-4 data. Then the total impulse calculation was optimized (by changing one of the waveform parameters) to match the results of REFLECT-4. As with the overpressure model, these modifications have not significantly degraded the dynamic pressure versus time fit.

ACCURACY

Because the particular conditions at the surface reflecting the blast are critical in determining the resultant blast-wave characteristics, over-pressures (and other blast parameters) are somewhat less predictable than those of free-air bursts. Carpenter's data for ground distances are estimated to be reliable to within ±15%, for yields between 1 and 20,000kT. This may correspond to uncertainties in the overpressure as much as 30%, depending upon the height of burst. Figures for overpressure above 700 kPa are purely theoretical and are estimated to be reliable to within ±20%. Scaling for yields below 1 kT and scaled heights of burst between 50 and 300 meters has shown large errors corresponding to factors of 2 or 3 in effective yield.

The peak overpressure fits used are typically accurate to ±4% with a worst case of 11% when compared with Carpenter's data. The average error increases to about ±10% if the fits are extended to 350,000 kPa.

As noted before, the dynamic pressure fit was not based directly on data from Carpenter, but was derived using the overpressure fit and Rankine-Hugoniot theory. In fact, very little dynamic pressure experimental data exists. However, when compared with a major hydrocode program REFLECT-4, the dynamic pressure fit had an average difference of ±32%. When the data points used in the comparison were limited to the Mach region the average difference dropped to ±19%.

The pressure versus time fits (impulses and waveform profiles) also have been compared with the REFLECT-4 results. The overpressure total impulse was off in the worst case by about 20% and on the average by about ±10%. The overpressure positive phase duration comparison showed large differences: 40% in the worst case and ±15% on the average. The general tendency of the errors was to increase with scaled height of burst with the worst case occurring above 200 meters.

The discrepancies between REFLECT-4 and the dynamic pressure waveform fits are more compartmentalized; that is, the worst case errors tend to occur in well-defined regions. In comparing the dynamic pressure total impulse with the REFLECT-4 results, for scaled ground range less than 300 meters the average difference is in the 30% to 40% range, with errors of the order of 80% for HOB below 60 meters and as large as 60% for HOB above 200 meters. For scaled ground ranges greater than 300 meters, the average error is better than ±5%, with worst cases of about 15% for HOB below 60 meters.

The dynamic pressure positive phase duration was fit using the REFLECT-4 data. The largest differences occur for the region of scaled ground ranges less than 300 meters and for scaled heights of burst below 60 meters. In this region the

worst case error is about 35% and the average around 10%. Outside this region the difference decreases substantially. The worst case discrepancy is less than 8% and the average is better than 3%.

The accuracy of the Gauss-Legendre Quadrature (20 points) used to compute the impulse integrals has been compared extensively with that given by Simpson's rule using about 2000 time points per integral. The worst case error for partial and total impulses (dynamic pressure and overpressure waveforms) is found to be less than 1%.

SOURCES OF DATA

- Bleakney, W., and A. H. Taub, "Interaction of Shock Waves," Reviews of Modern Physics, Vol. 21, p. 584, October 1949.
- Carpenter, H. J., Height-of-Burst Curves, RDA letter to M. Atkins, E. E. Conrad, J. F. Moulton, Jr., E. Sevin, and G. W. Ullrich, dated 8 June 1978.
- DNA Effects Manual Number 1. Capabilities of Nuclear Weapon, Stanford Research Institute, (unpublished).
- Hikida, Shuichi, "Triple Point Path Fit (1 kt)," S-Cubed, Albuquerque, NM, letter to Tom Schroeder, Horizons Technology, Inc., dated 12 May 1982.
- Sachs, Dr. Donald, editor, EM-1 Air Blast Phenomena (Preliminary Version), Kaman Sciences Corporation KW-81-11U(R), 2 February 1981.
- Smiley, Robert F., J. Ray Ruetenik, and Michael A. Tomayko, REFLECT-4 Code Computations of 40 kT Nuclear Blast Waves Reflected from the Ground, Kaman Avidyne KA TR-201, 1 November 1982.
- Speicher, S. J., and H. L. Brode, Airblast Overpressure Analytic Expression for Burst Height, Range and Time Over an Ideal Surface, PSR Note 385, Pacific-Sierra Research Corporation, Los Angeles, CA, November 1981. (see appendix C, underline added by this author)
- Speicher, S. J., "PSR QUICK FIX Analytic Expression for Dynamic Pressure-Time versus Range, Burst Height, and Yield," Pacific-Sierra Research Corporation, Los Angeles, CA, letter to Horizon Technology, Inc., dated 20 June 1983.

OTHER REFERENCES

- Brode, H. L., Height-of-Burst Effects at High Overpressures, RAND Corporation, RM-6301-DASA, DASA 2506, July 1970.
- (redacted), Theoretical Descriptions of the Blast and Fireball for a Sea Level Megaton Explosion, RM-2248, The Rand Corporation, Santa Monica, CA, 1959.
- (redacted), Analytic Approximations to Dynamic Pressure and Impulse and Other Fits for Nuclear Blasts, PSR Note 529, Pacific-Sierra Research Corporation, Los Angeles, CA, 20 May 1983.
- Carpenter, H. Jerry, Overpressure Impulse HOB Curves, RDA letter to M. Atkins, J. Moulton, E. Sevin, G. Stockton, and G. Ullrich, dated 31 August 1976.

- Speicher, S. J., and H. L. Brode, Revised Procedure for the Analytic Approximation of Dynamic Pressure Versus Time, PSR Note 320, Pacific-Sierra Research Corporation, Los Angeles, CA, May 1980. (see appendix D and appendix E, underline added by this author)

2.1 Peak Pressure, Dynamic Pressure & Arrival Time and Mach Stem Formation Range & Triple Point Height

- Limits (Overpressure, Dynamic pressure & Time of arrival)
  - Y, Weapon yield, kT, 0.1-25,000
  - HOB, Height of burst, m, 0-4,000 $Y^{1/3}$
  - GR, Ground range, m, LM-4,000 $Y^{1/3}$, in which:

$$LM = \begin{cases} 0, & HOB \geqslant 25Y^{1/3} \\ 20 \cdot Y^{1/3}, & \text{otherwise} \end{cases} \tag{1}$$

- Limits (Mach Stem, Triple points)
  - Y, Same
  - HOB, Height of burst, m, 0-800 $Y^{1/3}$
  - GR, Ground range, m, LM-4,000 $Y^{1/3}$, $LM = max(XM, 20 \cdot Y^{1/3})$
- Outputs:
  - PAIR, Air-burst peak pressure, Pa
  - QAIR, Air-burst peak dynamic pressure, Pa
  - TAAIR, Air-burst time of arrival, s
  - XM, Mach stem formation range, m
  - HTP, Height of triple point, m
- Model:
  The scaled ground range, scaled height of burst and scaled slant range are:

$$SGR = \frac{GR}{Y^{1/3}} \tag{2}$$

$$SHOB = \frac{HOB}{Y^{1/3}} \tag{3}$$

$$SR = \sqrt{SGR^2 + SHOB^2} \tag{4}$$

  Defining a function $\Delta p_{DNA} < X >$ that represents the Defense Nuclear Agency (DNA) Standard 1-kiloton free-air overpressure curve:

$$\Delta p_{DNA} < X >= \frac{3.04 \times 10^{11}}{X^3} + \frac{1.13 \times 10^9}{X^2} + \frac{7.9 \times 10^6}{X\sqrt{\ln[\frac{X}{445.42} + 3 \cdot \exp(-\frac{1}{3}\sqrt{\frac{X}{445.42}})}} \tag{5}$$

  calculate α, Slant angle, Radians

$$\alpha = \arctan(SHOB/SGR) \tag{6}$$

let the free-air peak overpressure $\Delta p_{FREE} = \Delta p_{DNA} < SR >$, then:

$$T = \frac{340}{\Delta p_{FREE}^{0.55}} \tag{7}$$

$$U = (\frac{7,782}{\Delta p_{FREE}^{0.7}} + 0.9)^{-1} \tag{8}$$

$$W = (\frac{7,473}{\Delta p_{FREE}^{0.5}} + 6.6)^{-1} \tag{9}$$

$$V = (\frac{647}{\Delta p_{FREE}^{0.8}} + W)^{-1} \tag{10}$$

the regular/Mach region merge angle, α_m, in radians:

$$\alpha_m = \arctan(\frac{1}{T+U}) \tag{11}$$

the width of merge region, β, in radians:

$$\beta = \arctan(\frac{1}{T+V}) \tag{12}$$

$$s = \frac{\alpha - \alpha_m}{\beta} \tag{13}$$

s_o clamps s to $[-1, 1]$, inclusive.
the regular/Mach region switching parameter, used to merge Δp_{MACH} and Δp_{REG} terms, is given by the expression:

$$\sigma = 0.5 \cdot [\sin(\frac{\pi s_o}{2}) + 1] \tag{14}$$

Case 1, σ is equal to 0: do equations under Mach reflected region.
Case 2, σ is between 0 and 1: do equations for both types of region.
Case 3, σ is equal to 1: do equations for regular reflected region.

– Equations for Mach reflected region

$$A = \min(3.7 - 0.94 \cdot \ln(SGR), 0.7) \tag{15}$$

$$B = 0.77 \cdot \ln(SGR) - 3.8 - \frac{18}{SGR} \tag{16}$$

$$C = \max(A, B) \tag{17}$$

$$\Delta p_{MACH} = \frac{\Delta p_{DNA} < \frac{SGR}{2^{1/3}} >}{1 - C\sin(\alpha)} \tag{18}$$

Defining a function $n, g_s < X >$: the incident shock strength, ξ, is:

$$\xi = \frac{X}{101,325} + 1 \tag{19}$$

$$t = 10^{-12}(\xi)^6 \tag{20}$$

$$z = \ln(\xi) - \frac{0.47 \cdot t}{100 + t} \tag{21}$$

gamma behind the shock:

$$g_s < X >= 1.402 - \frac{3.4 \cdot 10^{-4} \cdot z^4}{1 + 2.22 \times 10^{-5} \cdot z^6} \tag{22}$$

the shock mu, μ_s, is:

$$\mu_s = \frac{g_s + 1}{g_s - 1} \tag{23}$$

mass density ratio across shock front is given by:

$$n < X >= \frac{1 + \mu_s \cdot \xi}{5.975 + \xi} \tag{24}$$

– Equations for regular reflected region:
the normal reflection factor:

$$R_n = 2 + 0.5 \cdot (g_s < \Delta p_{FREE} > +1)(n < \Delta p_{FREE} > -1) \tag{25}$$

$$f = \frac{\Delta p_{FREE}}{75,842} \tag{26}$$

$$D = \frac{f^6 \cdot (1.2 + 0.07 \cdot \sqrt{f})}{f^6 + 1} \tag{27}$$

$$\Delta p_{REG} = \Delta p_{FREE} \cdot [(R_n - 2) \cdot \sin^D(\alpha) + 2] \tag{28}$$

All three cases continue from here. Merging the regular and Mach region overpressure terms by means of a switching parameter, σ, gives the air-burst peak pressure:

$$PAIR = \sigma \cdot \Delta p_{REG} + (1 - \sigma) \cdot \Delta p_{MACH} \tag{29}$$

let $n_q = n < PAIR >$ the air-burst dynamic pressure is,

$$QAIR = 0.5 \cdot PAIR(n_q - 1)[1 - \sigma \sin^2(\alpha)] \tag{30}$$

then, x_m, the scaled Mach stem formation range is calculated:

$$x_m = \frac{SHOB^{2.5}}{5,822} + 2.09 \cdot SHOB^{0.75} \tag{31}$$

XM, the unscaled formation range is thus:

$$XM = x_m \cdot Y^{1/3} \tag{32}$$

Let:

$$S = (5.98 \times 10^{-5} \cdot SHOB^2 + 3.8 \times 10^{-3} \cdot SHOB + 0.766)^{-1} \tag{33}$$

$$h = 0.9 \cdot x_m - 3.6 \cdot SHOB \tag{34}$$

HTP, unscaled height of triple point is:

$$\mathrm{HTP} = \mathrm{S}[\mathrm{h} + \sqrt{\mathrm{h}^2 + (\mathrm{SGR} - 0.9 \cdot \mathrm{x_m})^2 - \mathrm{x_m^2}/100}] \cdot \mathrm{Y}^{1/3} \tag{35}$$

then find a scaling factor for slant range:

$$\nu = \begin{cases} 1 & \mathrm{SGR} \leqslant \mathrm{x_m} \\ 1.26 - 0.26 \cdot (\dfrac{\mathrm{x_m}}{\mathrm{SGR}}) & \text{otherwise} \end{cases} \tag{36}$$

let the scaled range $\mathrm{R} = \mathrm{SR}/\nu$, $\mathrm{ta_{AIR}} = \mathrm{ta} < \mathrm{R} >$, the free-air time of arrival equation gives $\mathrm{ta} < \mathrm{X} >$:

$$\mathrm{ta} < \mathrm{X} >= \frac{\mathrm{X}^2 \cdot (6.7 + \mathrm{X})}{7.12 \times 10^6 + 7.32 \times 10^4 \cdot \mathrm{X} + 340.5 \cdot \mathrm{X}^2} \tag{37}$$

therefore the unscaled air-burst time of arrival is:

$$\mathrm{TAAIR} = \mathrm{ta_{AIR}} \cdot \mathrm{Y}^{1/3} \cdot \nu \tag{38}$$

2.2 Overpressure Total Impulse

- Limits (Overpressure impulse & positive phase duration):
  - Y, Weapon yield, kT, 0.1-25,000
  - HOB, Height of burst, m, 0-4,000 $\mathrm{Y}^{1/3}$
  - GR, Ground range, m, LM-4,000 $\mathrm{Y}^{1/3}$, in which:

$$\mathrm{LM} = \begin{cases} 0, & \mathrm{HOB} \geqslant 25\mathrm{Y}^{1/3} \\ 20 \cdot \mathrm{Y}^{1/3}, & \text{otherwise} \end{cases} \tag{39}$$

  - IPTOTAL, Overpressure total impulse, Pa-s.
  - DPP, Positive phase duration, s

- Model:
clamping SHOB and SGR to be greater than 10^{-7}, defining time-independent waveform parameters:

$$\mathrm{s} = 1 - \frac{1}{1 + \dfrac{1}{4.5 \times 10^{-8} \cdot \mathrm{SHOB}^7}} - \frac{\dfrac{5.958 \times 10^{-3} \cdot \mathrm{SHOB}^2}{1 + 3.682 \times 10^{-7} \cdot \mathrm{SHOB}^7}}{1 + \dfrac{\mathrm{SGR}^{10}}{3.052 \times 10^{14}}} \tag{40}$$

$$\mathrm{f} = \mathrm{s}[\frac{2.627 \cdot \mathrm{ta_{AIR}^{0.75}}}{1 + 5.836 \cdot \mathrm{ta_{AIR}}} + \frac{2,341 \cdot \mathrm{ta_{AIR}^{2.5}}}{1 + 2.541 \times 10^6 \cdot \mathrm{ta_{AIR}^{4.75}}} - 0.216] \tag{41}$$

$$+ 0.7076 - \frac{3.077}{10^{-4} \cdot \mathrm{ta_{AIR}^{-3}} + 4.367} \tag{42}$$

$$\mathrm{g} = 10 + \mathrm{s}[77.58 - \frac{154 \cdot \mathrm{ta_{AIR}^{0.125}}}{1 + 1.375 \cdot \mathrm{ta_{AIR}^{0.5}}}] \tag{43}$$

$$\mathrm{h} = \mathrm{s}[\frac{17.69 \cdot \mathrm{ta_{AIR}}}{1 + 1,803 \cdot \mathrm{ta_{AIR}^{4.25}}} - \frac{180.5 \cdot \mathrm{ta_{AIR}^{1.25}}}{1 + 99,140 \cdot \mathrm{ta_{AIR}^{4}}} - 1.6] + 2.753 \tag{44}$$

$$+\frac{56\cdot \mathrm{ta}_{\mathrm{AIR}}}{1+1.473\times 10^{6}\cdot \mathrm{ta}_{\mathrm{AIR}}^{5}} \tag{45}$$

let:

$$\mathrm{t_o}=\frac{\ln(1,000\cdot \mathrm{ta}_{\mathrm{AIR}})}{3.77} \tag{46}$$

$\mathrm{dp}_{\mathrm{SURF}}$, scaled overpressure positive phase duration on the surface, is:

$$\mathrm{dp}_{\mathrm{SURF}}=[155\cdot\exp(-20.8\cdot \mathrm{ta}_{\mathrm{AIR}})+\exp(-\mathrm{t_o}^2+4.86\cdot \mathrm{t_o}+0.25)]\times 10^{-3} \tag{47}$$

$\mathrm{dp}_{\mathrm{UNMOD}}$, unmodified scaled overpressure positive phase duration is:[1]

$$\mathrm{dp}_{\mathrm{UNMOD}}=\mathrm{dp}_{\mathrm{SURF}}\cdot[1-(1-\frac{1}{1+4.5\times 10^{-8}\cdot \mathrm{SHOB}^{7}})\times(0.04+\frac{0.61}{1+\frac{\mathrm{ta}_{\mathrm{AIR}}^{1.5}}{0.027}})] \tag{48}$$

$\mathrm{dp}_{\Delta \mathrm{p}}$, the scaled overpressure positive phase duration, for all height of burst is:

$$\mathrm{dp}_{\Delta \mathrm{p}}=\mathrm{dp}_{\mathrm{UNMOD}}\cdot[1.16\cdot\exp(\frac{-|\frac{\mathrm{SHOB}}{0.3048}-156|}{1,062})] \tag{49}$$

DPP, the unscaled positive phase duration, is therefore derived:

$$\mathrm{DPP}=\mathrm{dp}_{\Delta \mathrm{p}}\cdot \mathrm{Y}^{1/3} \tag{50}$$

if SGR$<x_m$ or SHOB$>$116, the waveform of the overpressure is of a single peak, in which case $\mathrm{dt}=0$ and the following part is skipped.

– Factors exclusive to double peaks case: x_e approximates the point 2 peaks are equal

$$x_e=\frac{138.3}{1+\frac{45.5}{\mathrm{SHOB}}} \tag{51}$$

let e be the value of $|\frac{\mathrm{SGR}-x_m}{x_e-\mathrm{SGR}}|$ clamped to between 50 and 0.02 inclusive.

$$w=\frac{0.583}{1+\frac{2,477}{\mathrm{SHOB}^2}} \tag{52}$$

[1]This equation is especially troublesome. The in-software help file had a typo, expressing the result as:

$$\mathrm{dp}_{\mathrm{UNMOD}}=\mathrm{dp}_{\mathrm{SURF}}\cdot[1-(1-\frac{1}{1+4.5\times 10^{-8}\cdot \mathrm{SHOB}^{7}})]\times(0.04+\frac{0.61}{1+\frac{\mathrm{ta}_{\mathrm{AIR}}^{1.5}}{0.027}})$$

This made little sense, as it is equivalent to:

$$\mathrm{dp}_{\mathrm{UNMOD}}=\frac{\mathrm{dp}_{\mathrm{SURF}}}{1+4.5\times 10^{-8}\cdot \mathrm{SHOB}^{7}}\times(0.04+\frac{0.61}{1+\frac{\mathrm{ta}_{\mathrm{AIR}}^{1.5}}{0.027}})$$

The form presented in the main text involves rearranging the square bracket to justify not simplifying the two subtractions, and is not based on any physical intuition.

the first peak to second peak ratio is given by:

$$d = 0.23 + w + 0.27 \cdot e + e^5 \cdot (0.5 - w) \tag{53}$$

$$a = (d - 1) \cdot (1 - \frac{1}{1 + e^{-20}}) \tag{54}$$

dt denotes the approximate time separation between peaks:

$$dt = \max(\frac{SHOB \cdot (SGR - x_m)^{1.25}}{8.186 \times 10^5}, 10^{-12}) \tag{55}$$

$$v_o = \frac{SHOB^6}{2,445 \cdot (1 + \frac{SHOB^{6.75}}{3.9 \times 10^4}) \cdot (1 + 9.23 \cdot e^2)} \tag{56}$$

$$c_o = \frac{1.04 - \frac{1.04}{1 + \frac{3.725 \times 10^7}{SGR^4}}}{(a + 1) \cdot (1 + \frac{9.872 \times 10^8}{SHOB^9})} \tag{57}$$

In both case, for any time t such that $ta_{AIR} \leqslant t \leqslant ta_{AIR} + dp_{\Delta p}$, using the time-independent parameters computed in the previous equations are used to represent overpressure versus time.

let $dp = dp_{\Delta p}$, the positive phase duration, then:

defining Δp_t as a function of t,

- For the case of single peak:

$$b = [f \cdot (\frac{ta_{AIR}}{t})^g + (1 - f) \cdot (\frac{ta_{AIR}}{t})^h] \cdot (1 - \frac{t - ta_{AIR}}{dp}) \tag{58}$$

then:

$$\Delta p_t = PAIR \cdot b \tag{59}$$

- For the case of double peaks:

$$b = [f \cdot (\frac{ta_{AIR}}{t})^g + (1 - f) \cdot (\frac{ta_{AIR}}{t})^h] \cdot (1 - \frac{t - ta_{AIR}}{dp}) \tag{60}$$

g_a is the value

$$\frac{t - ta_{AIR}}{dt} \tag{61}$$

clamped to between 400 and 0.0001, inclusive.

$$v = 1 + \frac{v_o g_a^3}{g_a^3 + 6.13} \tag{62}$$

$$c = c_o \cdot (\frac{1}{g_a^{-7} + 0.923 g_a^{1.5}}) \cdot [1 - (\frac{t - ta_{AIR}}{dp})^8] \tag{63}$$

then:

$$\Delta p_t = PAIR \cdot (1 + a) \cdot (b \cdot v + c) \tag{64}$$

For either case, the dynamic pressure total impulse IPTOTAL is then numerically integrated from $\mathtt{ta}_{\mathrm{AIR}}$ to $\mathtt{ta}_{\mathrm{AIR}} + \mathtt{dp}$.

$$\mathrm{IPTOTAL} = Y^{1/3} \cdot \int_{x=\mathtt{ta}_{\mathrm{AIR}}}^{\mathtt{ta}_{\mathrm{AIR}}+\mathtt{dp}} \Delta p_x \; dx \tag{65}$$

The original software recommended a Gauss-Legendre Quadrature, although more modern numerical techniques should prove entirely sufficient.

2.3 Dynamic Pressure Total Impulse & Positive Phase Duration

- Limits (Dynamic pressure impulse & positive phase duration):
  - Y, Weapon yield, kT, 0.1-25,000
  - HOB, Height of burst, m, 0-750 $Y^{1/3}$
  - GR, Ground range, m, LM-4,000 $Y^{1/3}$, in which $\mathrm{LM} = \mathtt{max}(1.3 \cdot \mathrm{XM}, 80 \cdot Y^{1/3})$
- Outputs:
  - IQTOTAL, Dynamic pressure total impulse, Pa-s
  - DPQ, Dynamic pressure positive phase duration, s
- Model:

$$\mathrm{SHOB}_o = \frac{\mathrm{SHOB}}{0.3048} \tag{66}$$

$$\mathrm{SGR}_o = \frac{\mathrm{SGR}}{0.3048} \tag{67}$$

$$\mathrm{SHOB}_x = |\mathrm{SHOB}_o - 200| + 200 \tag{68}$$

$$\mathrm{SGR}_x = \mathrm{SGR}_o - 1,000 \tag{69}$$

$$\mathtt{dp}_o = 0.3 + 0.42 \cdot \exp(-\mathrm{SHOB}_x/131) \tag{70}$$

$$\mathtt{dp}_x = \begin{cases} \mathtt{dp}_o + 4.4 \times 10^{-5} \cdot \mathrm{SGR}_x & \text{if } \mathrm{SGR}_x > 0 \\ \mathtt{dp}_o + \mathrm{SGR}_x[\frac{1}{2,361} - \frac{|\mathrm{SHOB}_x - 533|^2}{7.88 \times 10^7}] & \text{else} \end{cases} \tag{71}$$

$\mathtt{dp}_q$, or the scaled dynamic pressure positive phase duration is:

$$\mathtt{dp}_q = \begin{cases} \mathtt{dp}_x & \text{if } \mathrm{SHOB}_o \geqslant 200 \\ \mathtt{dp}_x \cdot [1 + 0.2 \cdot \sin(\frac{\pi}{200} \cdot \mathrm{SHOB}_o)] & \text{else} \end{cases} \tag{72}$$

one additional dynamic pressure waveform parameter being:

$$\delta_o = \mathtt{max}(\frac{\mathrm{SHOB}_o^{1.52}}{16,330} - 0.29, 0) \tag{73}$$

the dynamic pressure waveform decay exponent is:

$$\delta = 2.38 \cdot \exp[-7 \times 10^{-7} \cdot |\mathrm{SHOB}_o - 750|^{2.7} - 4 \times 10^{-7} \cdot \mathrm{SGR}_o^2] + \delta_o \tag{74}$$

the dynamic pressure waveform multiplier is:

$$q_o = 0.5 \cdot [1 - \sigma \cdot \sin^2(\alpha)] \tag{75}$$

for any time t such that $ta_{AIR} \leqslant t \leqslant ta_{AIR} + dp_q$, Δp_t is then computed.
Let $n_q = n < \Delta p_t >$:

$$q_t = 0.5 \cdot \Delta p_t \cdot (n_q - 1) \cdot (\frac{\Delta p_t}{PAIR})^{\delta} \tag{76}$$

let $dp = dp_q$, the dynamic pressure total impulse is then integrated thus:

$$IQTOTAL = Y^{1/3} \cdot \int_{t=ta_{AIR}}^{ta_{AIR}+dp} q_t \ dt \tag{77}$$

3 Freeair Models

The models were accurately reproduced.

Free-air calculations describe the properties of a blast wave in an infinite homogeneous atmosphere. Use of them for bursts near the earth is justified in circumstances where the reflected shock from the ground-air interface is irrelevant. They are the only calculations offered by the program for targets not on the ground. The program uses the 1-kT sea-level free-air Blast Standard relationship adopted by the Defense Nuclear Agency (DNA) to obtain peak overpressure from distance (slant range). Overpressure is then used in the general-case Rankine-Hugoniot relations, along with an accurate fit to shock gamma as a function of shock strength, to obtain dynamic pressure, shock density ratio, the shock normal reflection factor, and shock-front and peak particle Mach numbers. Time of arrival is obtained from an accurate curve fit, rather than by integrating reciprocal velocity.

Yield scaling for blast effects is accurate over many orders of magnitude, but only in regions where effects dependent on specific weapon characteristics or radiation are unimportant, for they upset the similarity arguments on which the scaling depends. This is reasonably assured by the model limits of the program.

Altitude scaling uses the U. S. Standard Atmosphere 1962 model. It is known empirically to be better to use the target altitude rather than the burst altitude when these differ ("modified Sachs scaling"). If the ratio of the mass density of air to the sea-level value of 1.225 kg/cubic meter is known, altitude in meters can be found from the equation

$$\text{altitude} = 44,400 \cdot [1 - (\text{density ratio})^{0.235}] \tag{78}$$

which is valid for altitudes less than 11,000 m or density ratios greater than 0.297.

ACCURACY Yield scaling contributes negligible error within model limits. The altitude scaling factors represent the model atmosphere accurately to 20km, and can be used to 32 kilometers without introducing errors greater than 1%. This is unimportant compared with error due to neglect of changing "blast efficiency," the fraction of yield represented by the blast wave, and other errors of altitude scaling.

The DNA 1-kT Standard overpressure-distance function agrees well with experimental data. For scaled ranges up to 300 meters, corresponding to sea-level overpressures above 50 kPa, values of peak overpressure are estimated to be accurate within $\pm$15 percent. For scaled distances greater than 300 meters, the estimate is $\pm$30 percent. It should be noted that for overpressures greater than about 100,000 kPa, corresponding to scaled ranges less than about 15 meters, use of the DNA 1-kT Standard (or any standard) can lead to error because the specific weapon characteristics may dominate the blast environment.

Time of arrival is estimated to be within $\pm$15 percent of the true value. Values of peak dynamic pressure, shock density ratio, and shock-front and peak particle Mach numbers are believed to be accurate to within a few percent when calculated from peak overpressure as the input. If the input variable is range, then the much larger uncertainties of the range-overpressure relationship are introduced, and may amount to 15 to 30 percent.

The shock normal reflection factor is calculated from incident peak overpressure also, with simplified Rankine-Hugoniot relations that use the value of gamma

behind the incident shock for air ahead of it and for air behind the reflected shock also. Comparison with better calculations shows that this leads to no errors greater than about 5 percent within the model limits, the largest errors occurring near 30,000 kPa incident overpressure.

SOURCES OF DATA

- Bleakney, W., and A. H. Taub, "Interaction of Shock Waves," Reviews of Modern Physics 21, 584 (1949).
- DNA Effects Manual Number 1. Capabilities of Nuclear Weapons, Stanford Research Institute, (unpublished).
- Needham, C. E., et al., Nuclear Blast Standard (1 kt), AFWL-TR-73-55, Air Force Weapons Laboratory, NM, 1973. (Latest equivalent formulation of the overpressure-distance relationship is in DNA 5648T, January 1981).

OTHER REFERENCES

- Brode, H. L., Height-of-Burst Effects at High Overpressures, RAND Corporation, RM-6301-DASA, DASA 2506, July 1970.
- Nuclear Weapons Blast Phenomena, Defense Atomic Support Agency,(unpublished).

3.1 Altitude Scaling Factors

- Limits:
  - ALT, altitude, m: 0-25,000
- Outputs:
  - SP: altitude scaling factor for pressure
  - SD: altitude scaling factor for distance
  - ST: altitude scaling factor for time
  - C: altitude dependent speed of sound
- Models:
  - for $0 \leqslant \mathrm{ALT} < 11,000$, the altitude scaling sub factors are:

$$\mathrm{T} = 1 - \frac{\mathrm{ALT}}{\sqrt{2 \times 10^9}} \tag{79}$$

$$\mathrm{P} = \mathrm{T}^{5.3} \tag{80}$$

  - for $11,000 \leqslant \mathrm{ALT} < 20,000$:

$$\mathrm{T} = 0.7537 \cdot [1 + 2.09 \times 10^{-7} \cdot \mathrm{ALT}] \tag{81}$$

$$\mathrm{P} = \sqrt{1.6} \cdot [1 + 2.09 \times 10^{-7} \cdot \mathrm{ALT}]^{-754} \tag{82}$$

  - for $20,000 \leqslant \mathrm{ALT}$:

$$\mathrm{T} = 0.684 \cdot [1 + 5.16 \times 10^{-6} \cdot \mathrm{ALT}] \tag{83}$$

$$\mathrm{P} = 1.4762 \cdot [1 + 5.16 \times 10^{-6} \cdot \mathrm{ALT}]^{-33.6} \tag{84}$$

The altitude scaling factors for pressure, distance and time, as well as the altitude-dependent speed of sound are:

$$\mathrm{SP} = \mathrm{P} \tag{85}$$

$$\mathrm{SD} = \mathrm{SP}^{-1/3} \tag{86}$$

$$\mathrm{ST} = \frac{\mathrm{SD}}{\sqrt{\mathrm{T}}} \tag{87}$$

$$\mathrm{C} = 340.5 \cdot \frac{\mathrm{SD}}{\mathrm{ST}} \tag{88}$$

3.2 Overpressure, Dynamic pressure & Time of arrival

- Limits:
  - Y, weapon yield, kT, 0.1-25,000
  - ALT, altitude, m: 0-25,000
  - RANGE, range, m: $16 \cdot \mathrm{Y}^{1/3} \cdot \mathrm{SD} - 4,000 \cdot \mathrm{Y}^{1/3} \cdot \mathrm{SD}$
- Outputs:
  - PFREE: Free air peak overpressure, Pa
  - QFREE: Free air dynamic pressure, Pa
  - TAFREE: Free air time of arrival, s
- Models:

$$\mathrm{R} = \frac{\mathrm{RANGE}}{\mathrm{SD} \cdot \mathrm{Y}^{1/3}} \tag{89}$$

Let $\Delta\mathrm{P}_{\mathrm{FREE}} = \Delta\mathrm{P}_{\mathrm{DNA}} < \mathrm{R} >$

$$\mathrm{PFREE} = \Delta\mathrm{P}_{\mathrm{FREE}} \cdot \mathrm{SP} \tag{90}$$

Now, we have the free air peak dynamic pressure:

$$\mathrm{q}_{\mathrm{FREE}} = 0.5 \cdot \Delta\mathrm{P}_{\mathrm{FREE}} \cdot (\mathrm{n} < \Delta\mathrm{P}_{\mathrm{FREE}} > -1) \tag{91}$$

Scaling it to altitude:

$$\mathrm{QFREE} = \mathrm{q}_{\mathrm{FREE}} \cdot \mathrm{SP} \tag{92}$$

$\mathrm{ta}_{\mathrm{FREE}}$ scaled free air blast wave time of arrival is:

$$\mathrm{ta}_{\mathrm{FREE}} = \mathrm{ta} < \mathrm{R} > \tag{93}$$

Un-scaling for altitude and weapon yield:

$$\mathrm{TAFREE} = \mathrm{ta}_{\mathrm{FREE}} \cdot \mathrm{ST} \cdot \mathrm{Y}^{1/3} \tag{94}$$

4 Initial Radiation Models

The objective of this calculation is to calculate the total initial radiation dose near the ground in tissue and in silicon for 13 generic weapon types (shown on the next three pages) as functions of weapon yield, height of burst, ground range, relative air density, fission fraction, and of the weapon type. Total dose is the sum of the neutron dose, secondary gamma-ray dose, and dose from fission-fragment gamma rays. Initial radiation dose is defined to be that accumulated within the first minute after the burst.

The relative air density (relative to normal sea-level air density of 1.225 milligrams per cubic centimeter) to be used should consider the altitudes of the weapon and of the point at which the dose is absorbed.

If those altitudes are not the same, find the relative air densities for both, and use the average. The relationship between altitude (in meters) and relative air density is given by:

$$\texttt{relative air density} = \exp[-(\texttt{altitude})^{1.04}/13,800] \tag{95}$$

This equation is valid to an altitude of approximately 7,000 meters.

Table of Yield Range for Various Weapon Types

WT	Description	Yield Range (kT)	
1	Gun assembled fission weapon	0.1	few tens
2	Older boosted or un-boosted fission implosion weapon	1	few tens
3	Contemporary un-boosted fission implosion weapon	less than 1	
4	Contemporary boosted fission implosion weapon	1	few tens
5	Modern boosted fission implosion weapon	1	few tens
6	Un-boosted fission implosion	less than 1	
7	Boosted fission implosion	1	10
8	Single yield thermonuclear	few tens	5000
9	Multiple yield thermonuclear: high option	100	500
10	Multiple yield thermonuclear: low option	few tens	
11	Tactical (clean) thermonuclear	few tens	few hundreds
12	Thermonuclear: very high yield	greater than 5000	
13	Enhanced radiation	Unspecified	

for type 13, user familiarity with specific applications is required for meaningful results.

Only such gross aspects of initial nuclear radiations as received dose can be predicted to useful accuracy by simple methods. The model, from the data source document, corrects for ambient density variations using mass-integral scaling. It also corrects for the receiver being at 1.5 meters above smooth earth, and for finite height of burst. For the fission-fragment gamma-ray component it applies a further hydrodynamic enhancement factor to account for rise of the fission fragments in the fireball and for shock-induced changes in density.

There are some minor differences between this calculation and the original form of the data presented in the source document. These differences were introduced as needed to eliminate some discontinuities that might otherwise exist, and to enable calculation of all radiation sources within the model limits. The overall accuracy of the results is not affected.

The fission fragment gamma dose calculation is based upon ATR 4.1 data as modified by Science Applications, Inc. (SAI) for yields below 1 MT. All other dose

calculations are based on DNA's Effects Manual Number 1. Prompt gamma rays have been neglected here, since their contribution to the total dose is not significant.

ACCURACY

The source document gives very little data on which to determine the typical error of the total dose calculation. It is, however, possible to give individual estimates of the calculation errors (i.e. the precision with which this program matches the data source) for the neutron, secondary gamma and fission fragment gamma doses.

For the model limits (see MODEL AND ABSOLUTE LIMITS under RELATED TOPICS)(reproduced below) the neutron dose is typically accurate to ±6% with a worst case of about 30%. The secondary gamma dose has an average error of ±8% and a worst case error of 40%. For the fission fragment dose component the typical error is about ±20%. These error estimates are only accurate for component doses larger than about 1 rad(tissue). For the neutron and secondary doses, the error estimates are valid for the ground range limit discussed in MODEL AND ABSOLUTE LIMITS.

The source document claims errors for the neutron and secondary gamma dose components data are roughly ±70%, but says there are instances where the errors can be much larger. The uncertainty in the fission fragment dose is roughly a factor of 2 for weapon yields less than 100 kT, and as great as 5 for yields greater than 10 MT. Consult the source document if available, for a more detailed account of the errors.

The source recommends that for bursts over sea-water that the neutron dose be reduced by 30% and the secondary gamma dose be doubled. It is recommended that the weapon yield not be made smaller than 0.01kT nor larger than 50 MT.

SOURCES OF DATA

- Dolan, Philip J., editor, Capabilities of Nuclear Weapons(U), Stanford Research Institute, DNA Effects Manual Number 1, Part I, Chapter 5(S/RD) by Science Applications, Inc. (unpublished).
- Huszar, L., W. A. Woolson and E. A. Straker, Version 4 of ATR (Air Transport of Radiation) Science Applications, Inc., January 1976.

4.1 Initial radiation

The model is reproduced save for rounding artefact on the least significant digit.

- Inputs & Limits:
  - Y, weapon yield, kT, 0.01kT - 25MT
  - AIR, air density ratio, 1, 0.6 - 1.0
  - H, height of burst, m, $1.5/\mathrm{AIR} - 10,000/\mathrm{AIR}$
  - GR, ground range, m, $x/\mathrm{AIR} - y/\mathrm{AIR}$, where:[2]

$$x = \begin{cases} \sqrt{\max(0, 10^4 - H^2)} & \text{N and SG doses} \\ \sqrt{\max\{0, [150 \cdot \max(1, Y^{1/3})]^2 - H^2\}} & \text{all other} \end{cases} \tag{96}$$

$$y = \sqrt{10^8 - H^2} \tag{97}$$

[2]This part conforms to the documentation *Model Limits* rather than the model description, as it appears to be the correct form.

  - FF, fission fraction, 1, 0 - 1
  - WT, weapon type. 1 - 13.

- Outputs:
  - N, neutron component of total dose, rad (tissue)
  - SG, secondary-gamma component of total dose, rad (tis)
  - FFG, fission-fragment-gamma component of total dose, rad (tis)
  - TD, total dose, rad (tis)
  - DS, total dose, rad (silicon)
  - N/G, neutron-to-gamma dose ratio

- Models:
  The component doses are:

$$N = D_n \cdot C_n \cdot Y \cdot AIR^2 \tag{98}$$

$$SG = D_g \cdot C_g \cdot Y \cdot AIR^2 \tag{99}$$

$$FFG = D_{ff} \cdot C_f \cdot H_e \cdot Y \cdot FF \tag{100}$$

$$\tag{101}$$

  and the total dose (in tissue) is the sum of the components:

$$TD = N + SG + FFG \tag{102}$$

  the slant range is

$$SR = \sqrt{GR^2 + H^2} \tag{103}$$

  air-density scaled slant range

$$SR_o = AIR \cdot SG \tag{104}$$

  air-density scaled height of burst

$$H_o = AIR \cdot H \tag{105}$$

  height of burst switching parameter for C_g and C_n:

$$s = \min[1, \max(-1, \frac{H_o - 277}{50})] \tag{106}$$

$$\sigma = 0.5 \cdot [1 + \sin(\frac{s\pi}{2})] \tag{107}$$

  - Neutron dose yield-scaled factor: [3]

[3]The coefficients are exactly reproduced from the file WE.BEG, which is believed to be the data file for the program WE.EXE. These differ slightly from the documentation, and the documented coefficients have been included inside brackets wherever applicable. It is unclear which one was intended.

$$D_n = \frac{a}{(SR_o)^c} \cdot \exp(b \cdot SR_o) \quad (108)$$

where:

$$a = 10^6 \cdot a' \quad (109)$$

$$b = -\frac{500 + b'}{10^5} \quad (110)$$

$$c = 1 + \frac{c'}{1000} \quad (111)$$

the coefficients a', b', c' for D_n:

Coefficients for D_n			
WT	a'	b'	c'
1,3	253	71	138
2	98	49	225
4,7,11	394	31	261
5	347	52	147
6	177	67	152
8	450	24	323
9	753	-13	492 (482)
10	272	13	933
12	300	-13	492
13	1431	-2	63

– Secondary-gamma dose yield-scaled factor:

$$D_g = \frac{a}{(SR_o)^c} \cdot \exp[b \cdot (SR_o)^d] \quad (112)$$

where for $WT = 10$:

$$a = 13.5, \quad b = -0.344, \quad c = -1.537, \quad d = 0.5173 \quad (113)$$

for all other WT:

$$a = 10^{a'/100} \quad (114)$$

$$b = -\frac{193 + b'}{10^4} \quad (115)$$

$$c = \frac{c'}{1,000} \quad (116)$$

$$d = 0.8 \quad (117)$$

the coefficients a', b', c' for D_g:

Coefficients for D_g			
WT	a'	b'	c'
1	357	32	-188
2	605	0	793
3,6	433	27	68.8
4,5,7,9,11	542	14	439
8	490	18	297
12	604	7	633
13	722	8	651

– Fission-fragment-gamma dose yield-scaled factor:

$$D_{ff} = \frac{1.42 \times 10^7}{(SR_x)^{0.9516}} \cdot \exp[\frac{-(SR_x)^{0.774}}{32.7}] \quad (118)$$

where:

$$SR_x = sign(SR - 140) \cdot |SR - 140|^p + 140 \quad (119)$$

the $sign$ function is simply:

$$sign(x) = \begin{cases} -1, & x < 0 \\ 0, & x = 0 \\ +1, & x > 0 \end{cases} \quad (120)$$

and:

$$p = AIR \cdot (0.264 - AIR/12.6) + 0.815 \quad (121)$$

– Secondary gamma dose height of burst correction factor is:

$$C_g = a + \exp\{b + c \cdot [1 - \exp(4 \times 10^{-5} \cdot SR_o)]\} \tag{122}$$

where:

$$H_x = \min(1000, H_o) \tag{123}$$

for $WT = 13$:

$$\begin{cases} C_{gmax} = 1.1 \\ a_o = 0.002 \\ b = -2.12 + \exp(\dfrac{H^{0.903}}{204}) + 0.977 \cdot (1 - \sigma) \end{cases} \tag{124}$$

and for all other WT:

$$\begin{cases} C_{gmax} = 1 \\ a_o = 0.0035 \\ b = \dfrac{b'}{100} + \exp(\dfrac{H_x^{0.88}}{b'' + 192}) + \dfrac{(1 - \sigma) \cdot \pi}{6} \end{cases} \tag{125}$$

for all WT:

$$x = 0.9 - \frac{a'}{1,000} \tag{126}$$

$$t_1 = a_o \cdot H_o^x \tag{127}$$

$$t_2 = a_o \cdot (277)^x + 0.00011 \cdot H_o^{(1+a''/100)} \tag{128}$$

$$a = \min[C_{gmax}, 0.31 + (1 - \sigma) \cdot t_1 + \sigma \cdot t_2] \tag{129}$$

$$c = c' + \frac{\sigma}{c''} \cdot [\max(0, H_x - 277)]^{1.4} \tag{130}$$

and the coefficients $a', a'', b', b'', c', c''$ for C_g are as follows:

Coefficients for C_g						
WT	a'	a''	b'	b''	c'	c''
1,3,4	59	9	8	5	98	108
2,6,10	61	9	34	13	108	142
5	50	11	-25	1	90	92
7,12	42	12	-4	2	100	93
8,9,11	44	11	-43	0	86	87
13	-87	12	0	0	62	54(84)

– Fission fragment gamma dose correction factor:
Based on ATR 4.1 data as modified by SAI for yields below 1Mt:
The yield scaled height of burst[4]

$$SH = \min(\frac{H}{Y^{1/3}}, 250) \tag{131}$$

$$s_f = \sin[1.16 \cdot \log_{10}(Y) - 1.39] \tag{132}$$

[4]Examples from DNA EM-1 Capabilities of Nuclear Weapons supports that the documentation erroneously took the maximum instead of the minimum for SH

$$z = \frac{\log_{10}(Y) - 1.4}{3.5} \tag{133}$$

$$C_f = 0.5 \cdot (z + \sqrt{z^2 + 0.044}) \cdot AIR \cdot (1 - \frac{SH}{125}) + 0.038 \cdot \log_{10}(Y) - 0.22$$

$$+ [\frac{GR}{1,000} - 0.65 \cdot \log_{10}(Y) - 0.4] \cdot 0.075 \cdot [s_f + 2 \cdot |s_f| \cdot (AIR - 0.9)] \tag{134}$$

then:

$$C_f = 10^{C_f} \tag{135}$$

– Fission fragment gamma dose hydrodynamic enhancement factor:
For Y less than 1 do:

$$H_e = 1 \tag{136}$$

otherwise for $Y \geqslant 1$:

$$A_H = 10^{a \cdot [\log_{10}(Y)]^b} \tag{137}$$

where

$$a = 0.1455 \cdot AIR - 0.0077 \tag{138}$$

$$b = 2.55 - 0.35 \cdot AIR \tag{139}$$

and

$$B_Y = 1 - \{1 + c \cdot [\log_{10}(Y)]^{2.6}\} \cdot \exp\{-d \cdot [\log_{10}(Y)]^{2.6}\} \tag{140}$$

where:

$$c = 0.05875 \cdot AIR + 0.004 \tag{141}$$

$$d = 0.04 \cdot AIR - 0.03 \cdot sign(AIR - 0.6) \cdot |AIR - 0.6|^{1.3} \tag{142}$$

finally:

$$H_e = \min[A_H \cdot \exp(\frac{B_Y \cdot SR}{1,000}), \exp(SR \cdot \frac{-0.26 + 2.563 \cdot AIR}{1,000})] \tag{143}$$

– Neutron dose height of burst correction factor:

$$C_n = a + b \cdot \exp[-c \cdot (SR_o)^d] \tag{144}$$

where:

$$t_1 = 0.205 + 2.2 \times 10^{-3} \cdot H_o^{0.839} \tag{145}$$

$$t_2 = 0.4514 + \frac{H_o^{1.636}}{637^2} \tag{146}$$

$$a = \min[1, (1 - \sigma) \cdot t_1 + \sigma \cdot t_2] \tag{147}$$

$$t_3 = 0.388 + 0.116 \cdot H_o^{0.27} \tag{148}$$

$$t_4 = 0.9176 + \frac{H_o^{3.726}}{1.78 \times 10^{10}} \tag{149}$$

$$b = (1 - \sigma) \cdot t_3 + \sigma \cdot t_4 \tag{150}$$

$$c = 8 \times 10^{-4} + \frac{0.728}{H_o^{1.23} + 23.6} \tag{151}$$

$$d = 0.9 \tag{152}$$

if $H_o > 1$ then[5]

$$d = d + \frac{\ln(H_o)}{25} \tag{154}$$

N/G, the neutron dose/gamma-ray dose ratio is:

$$N/G = \frac{N}{SG + FFG} \tag{155}$$

The total dose in silicon is:

$$DS = FFG + SG + f_n \cdot N \tag{156}$$

in which:

$$f_n = \begin{cases} 0.015 & \text{WT neither 10 nor 13} \\ \dfrac{\exp(\frac{SR}{800})}{250} & WT = 10 \\ \dfrac{\exp(-\frac{SR}{234.7})}{20} + \dfrac{\exp(-\frac{SR}{4,329})}{25} & WT = 13 \end{cases} \tag{157}$$

[5]Through extensive testing, it has been determined that the actual implemented form is detailed as above. The repeat of the factor 0.9 in the original documentation:

$$d = d + 0.9 + \frac{\ln(H_O)}{25} \tag{153}$$

is likely a typo

5 Thermal Fluence Models

This program calculates the thermal fluence (time-integrated flux) received by a target on the ground and facing a nuclear burst, as a function of yield, height of burst, ground range and visibility.

Visibility is a subjective measure of air transmission described as `the distance at which a large dark object is just recognizable against the sky background' in daylight and as `the largest distance at which one can see an unfocused light of moderate intensity' at night. The target is assumed to be oriented normal to the source. The time integration used here extends only to a time equal to ten times the time of second maximum of the thermal output.

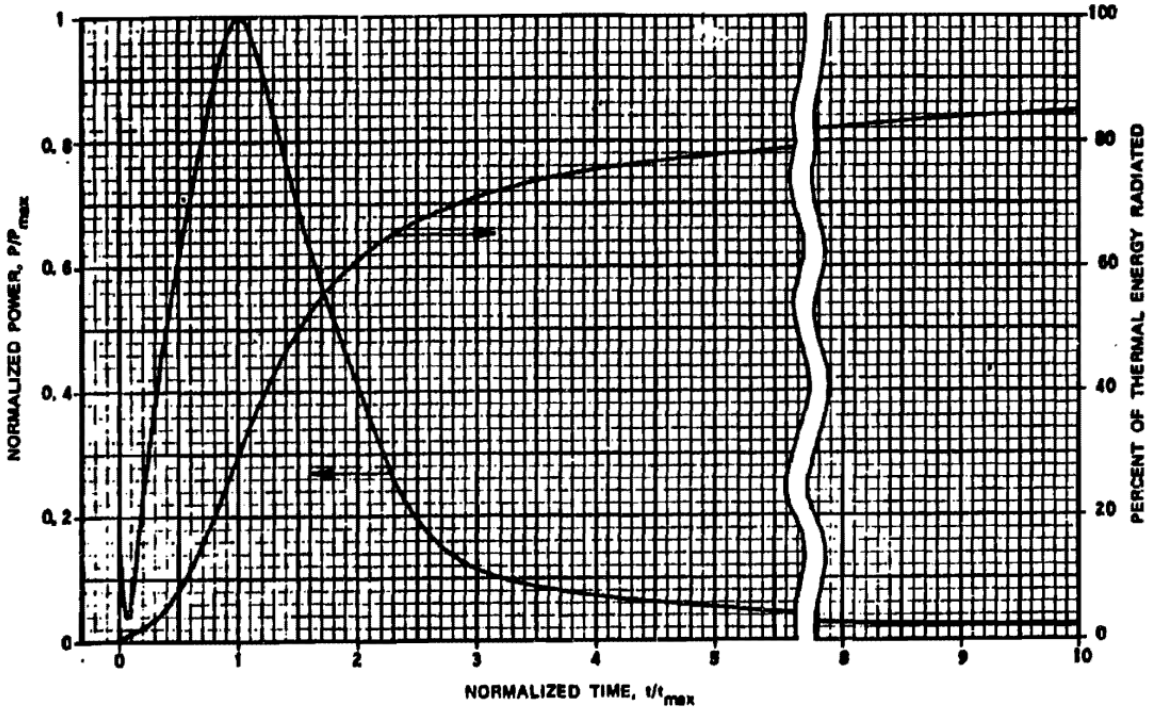

Figure 3-20. Power-Time and Energy-Time Curves for a 200 kiloton Burst at 5,000 feet

Figure 1: Capabilities of Nuclear Weapons (1972), Dolan, Philip J., (Ed) Defense Nuclear Agency Effects Manual Number One, section 3-48, figure 3.20, page unavailable.

When a nuclear burst occurs at the surface, or low enough for its fireball to touch the surface before the time of shock formation, surface material is mixed into the fireball air and lowers its temperature. This reduces the fraction of the yield that appears in the thermal pulse and extends the time over which it is delivered. Consequently, the fluence as defined here is much less than that from a low air burst at the same yield. The effect is most pronounced for low yields.

No allowance has been made here for the effects of reflections from clouds or from the surface. Cloud cover can increase measured fluence by 20% to 30%, and it is estimated that a combination of cloud cover and a covering of snow or light-colored sand on the earth's surface can increase it by as much as 250%. You should be aware of these possibilities in applications of this program.

ACCURACY:

The thermal fluence fit used is accurate to ±5% in most cases with some instances of 10% errors when compared with the source data. Since there is little experimental data with which to compare the thermal fluence data, general statements of its accuracy are difficult to make. Consult the source documents if available for details on the accuracy of the data.
SOURCES OF DATA

- Dolan, Philip J.,Capabilities of Nuclear Weapons(U), Stanford Research Institute, DNA Effects Manual Number 1, July 1972, Part I, Chapter 3 (revision in publication).
- Rough Draft Revision of Chapter 3 of EM-1, Kaman Sciences Corporation K-82-79(R), 26 February 1982, revised 24 February 1983 (unpublished).
- Dr. Forrest R. Gilmore, private communication.

The aforementioned time of second maximum (also known as final maximum, technically the third maximum as the first two have been squeezed into the pulse at 0 normalized time) can be found by:

$$t_{max} = 0.043 \cdot W^{0.43} \cdot (\frac{\rho}{\rho_0})^{0.42} \quad \text{sec} \tag{158}$$

from the first source, section 3-49. Similarly, the maximum power

$$P_{max} = \frac{4.3 \cdot W^{0.6}}{(\frac{\rho}{\rho_0})^{0.44}} \quad \text{kT/sec} \tag{159}$$

5.1 Thermal Fluence Model

This model is reproduced without issue.

- Model Inputs and Limits:
  - Y, yield, kT, 0.1kT - 25MT
  - H, height of burst, m, 0-1500·$Y^{1/3}$
  - GR, ground range, m, x-2200·$Y^{1/3}$, where:

$$x = \sqrt{\max[(100 \cdot Y^{1/3})^2 - H^2, 0]} \tag{160}$$

  - VIS, visibility, m, 10,000 - 80,000
- Output:
  - FLUE, thermal fluence to ten times the time of second maximum of thermal output, cal/cm^2
- Models:
  The slant range:

$$SR = \sqrt{H^2 + GR^2} \tag{161}$$

  The transition height of burst:

$$H_T = 4 \cdot Y^{1/3} \tag{162}$$

– Equations for surface burst:

$$A_1 = 0.32 \cdot [1 - \exp(-12 \cdot Y^{-VIS/17{,}000})] \tag{163}$$

$$B_1 = -\frac{\log_{10}(Y)^2}{275} + 0.0186 \cdot \log_{10}(Y) - \frac{1}{40} \tag{164}$$

$$A_2 = [(30 \cdot Y^{-0.26})^4 + 1350]^{-1/4} \tag{165}$$

$$B_2 = -(\frac{1.457}{VIS} + 9.3 \times 10^{-6}) \tag{166}$$

$$F_S = A_1 \cdot \exp(B_1 \cdot SR) + A_2 \cdot \exp(B_2 \cdot SR) + 0.006 \tag{167}$$

– Equations for air burst:

$$A_3 = \frac{H^{3/2}}{5 \times 10^7} + \frac{97}{281 + \sqrt{Y}} \tag{168}$$

$$B_3 = \frac{0.139}{H} \cdot [\exp(\frac{-8 \cdot H}{VIS}) - 1] \tag{169}$$

$$F_A = A_3 \cdot \exp(B_3 \cdot SR) \tag{170}$$

Although the result for ground burst is of limited value, it is noted that the model limit does include the case where $H = 0$, so the divide by zero in factor B3 in this case is probably unintended and can be avoided by taking $\lim_{H \to 0} B3 = -1.112/VIS$.

– Equations for transition region:

$$F = \begin{cases} F_A, & H \geqslant H_T \\ F_A \cdot (\frac{H}{H_T}) + F_S \cdot (1 - \frac{H}{H_T}), & 0 \leqslant H < H_T \end{cases} \tag{171}$$

$$Q = 8 \times 10^6 \cdot F \cdot \frac{Y}{SR^2} \tag{172}$$

Finally:

$$FLUE = Q \tag{173}$$

6 Cratering

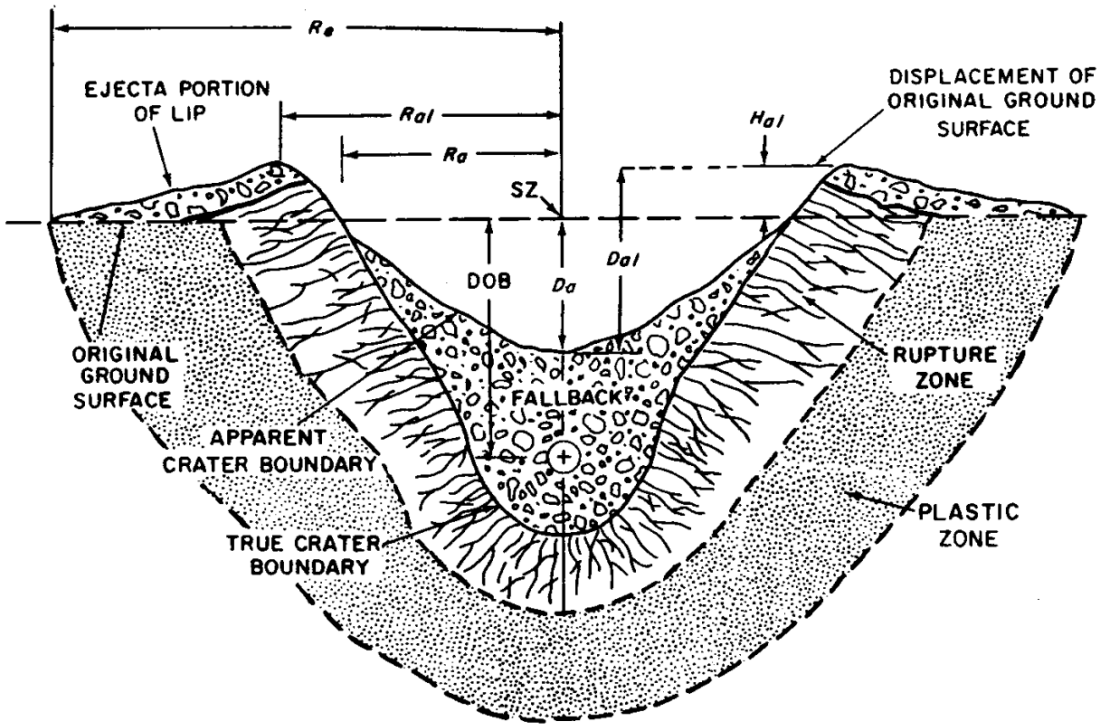

Figure 2: Effects of Nuclear Weapons (1977), Glasstone, S., Dolan, Philip J., section 6, figure 70, page 254.

The objective of these calculations is to determine the `best estimate' apparent volume, radius and depth of craters formed by near surface and deeply buried nuclear bursts. The bursts are assumed to occur near stratified media of up to three layers whose composition can be selected from five generic material types.

The bowl-shaped craters that are calculated are to be considered `lethal' craters, appropriate to the time of initial crater formation. After a period of time, particularly for we media and large yields, the shape may become more `dish-like', due to subsidence of the fallback material.

Cratering coefficients are greater for low-yield weapons than for high (greater than 20kT). For the NORMAL RADIATION cratering calculation, the program interpolates in the 1-20kT region to provide a smooth transition. If a weapon of less than 20kT is known to have a high radiative output, the HIGH RADIATION option should be used. This option attributes to the low yield weapon the low cratering efficiency it would have if it were of a high yield.

Layers are specified by entering a material composition and thickness for each layer. The bottommost is assumed to have semi-infinite thickness. The crater volume is calculated for each layer separately, as if it alone were the only layer present; then an average volume is computed using the single-layer volumes and a special iterative method. The crater radius, depth and ejecta calculations are based on the average volume.

The structure of calculation is such that a three-layer medium is assumed. If only a one- or two-layer calculation is desired, the geological material type for the unwanted layers must be specified as `NO LAYER PRESENT'....

The `best estimate' volume curves in the source document are within approximately a factor of 5 of the upper and 2.5 of the lower curves bounding the data. The accuracy of the radius and depth calculations is approximately ±45%. Assumptions inherent in the averaging method used for layered media will increase these uncertainties for these cases. It is best to consult the source document if available for more detail regarding the accuracy of these calculations.

SOURCE OF DATA

- Dolan, Philip J., editor, Defense Nuclear Agency Effects Manual Number 1. Capabilities of Nuclear Weapons, Part I: Phenomenology Section II: "Cratering Phenomena", Part 1, Change 2, 1 August 1981, Stanford Research Institute (unpublished).
- Lewis, John, R & D Associates, letters to the Defense Nuclear Agency, dated 25 August 1983 and 12 October 1983 (unpublished).
- Moore, Jeffrey, and Binky Lee, "A Proposed Interpolation Method for Determining Crater Volumes between 1 kT to 10 kT in EM1," R & D Associates, 21 August 1981 (unpublished).
- Port, Robert, R & D Associates, letter to the Defense Nuclear Agency dated 24 September 1981 (unpublished).
- Robert, R & D Associates, letter to the Defense Nuclear Agency dated 95024 September 1981 (unpublished).

6.1 Cratering

The cratering models were reproduced. The original document left something to be desired in regards to clarifying the exact procedure. An issue with the original implementation is that the ejecta thickness EJ is always calculated using the material type modifier of the topmost layer and the averaged volume. In our work, we have elected to use a weighted average of the calculated ejecta thickness for each layer, using the same weights as for the average crater volume. This (surprisingly) gave almost-matching (to within less than 1%) result for the case where all layers are of the same material, and slightly deviating result for the case where layers are composed of differing materials.

The model detailed in the documentation did not provide for differing types of weapon yield model below 1kT. However, the actual implementation in WE differentiates between HIGH RADIATION and NORMAL RADIATION for all yields less than 20kT. Therefore the form documented below has been slightly modified to take account of such.

- Inputs and Limits:
  - Y, yield, kT, $0.1 \leqslant Y \leqslant 25{,}000$
  - H, height of burst, m, $-40 \cdot Y^{1/3} \leqslant H \leqslant 3 \cdot Y^{1/3}$ (for dry soil the actual limit is $H \leqslant 3 \cdot Y^{1/3.1}$)
  - $T_1 - T_2$, thickness of layer 1-2, m, $0 \leqslant T_n \leqslant 1000$. Layer 3 is simply semi-infinite.
  - $M_1 - M_3$, geologic material types, $1 \leqslant M_n \leqslant 5$, where:

M_n	material type
1	dry soil
2	wet soil
3	dry soft rock
4	wet soft rock
5	hard rock

  - GR, ground range from burst point, m, $1.8 \cdot CR \leqslant GR \leqslant 10{,}000$
  - HIGH RADIATION, flag denoting if the weapon has high radiation output.

- Outputs:
  - V, apparent crater volume, m^3
  - CR, apparent crater radius, m
  - CD, apparent crater depth, m
  - EJ, depth of ejecta or debris, m
- Model:

  For each layer, the first and second scaled depth of burial is:

$$\mathsf{S}_1 = -\frac{\mathsf{H}}{\mathsf{Y}^{1/3}} \tag{174}$$

$$\mathsf{S}_2 = -\frac{\mathsf{H}}{\mathsf{Y}^{\alpha}} \tag{175}$$

  where the volume scaling exponent α varies with material type, and burst location. The latter falls into 3 regions, air burst, near surface buried, and deeply buried. The yield also falls into 3 regions: 1kT or less, 1-20kT (interpolation region), and greater than 20kT. Weapons with high radiative output use the 20kT scaling exponent for all yields. Normal radiative output weapons use an interpolation in the 1 to 20kT region.

  - all material types, $\mathsf{Y} < 1\text{kT}$

$$\alpha_1 = \begin{cases} (3)^{-1}, & -3 \leqslant \mathsf{S}_1 \leqslant 0.15 \\ 0.2946 + \dfrac{\exp[-\mathsf{S}_1 \cdot \log_{10}(583)]}{\sqrt{305}}, & 0.15 \leqslant \mathsf{S}_1 \leqslant 5 \\ (3.4)^{-1}, & 5 \leqslant \mathsf{S}_1 \end{cases} \tag{176}$$

  - all material types except dry soil, $\mathsf{Y} > 20\text{kT}$

$$\alpha_{20} = (3.4)^{-1} \tag{177}$$

  - dry soil, $\mathsf{Y} > 20\text{kT}$

$$\alpha_{20} = \begin{cases} (3.1)^{-1}, & -3 \leqslant \mathsf{S}_1 \leqslant 0 \\ [3.4 - 0.3 \cdot \exp(-2.2 \cdot \mathsf{S}_1)]^{-1}, & 0 \leqslant \mathsf{S}_1 \leqslant 5 \\ (3.4)^{-1}, & 5 \leqslant \mathsf{S}_1 \end{cases} \tag{178}$$

  and:

  - for Y >20kT, or if the weapon is HIGH RADIATION the exponent is:

$$\alpha = \alpha_{20} \tag{179}$$

  - otherwise:

$$\mathsf{g} = \begin{cases} 0, & \text{high radiation} \\ 1 - \min\{1, \max[0, \log_{20}(\mathsf{Y})]\}, & \text{low radiation} \end{cases} \tag{180}$$

    the interpolated α scaling exponent is:

$$\alpha = 3 \cdot [\alpha_{20} + \mathsf{g} \cdot (\alpha_1 - \alpha_{20})] \tag{181}$$

all of the above calculated values are held as constant, and a function $SV < y >$ is defined: (note y is solely used to choose the branch of calculation and not an actual parameter.)

- for all material types except dry soil, $Y > 20$kT:

$$SV = L/J \times 10^{K\cdot[\exp(F\cdot S_2+G\cdot S_2^2)-1]+D\cdot S_2}, \quad -3 < S_2 < 0.15 \tag{182}$$

where coefficients K, F, G, D, L:

Region	F	G	D	K	L
$y \leqslant 1$, buried	-1.05	-0.105	0.0573	-0.5	16989
$y \leqslant 1$, air	0.258	0.01	0.1	1.9	16989
$y \geqslant 20$, buried	-2	-0.3044	0.0707	-0.9059	5663
$y \geqslant 20$, air	0.53	0.028	-1/46	1.74	5663

and J:

Material Type	No.	J
dry soil ($y < 1$kT only)	1	4
wet soil	2	1
dry soft rock	3	5
wet soft rock	4	2
hard rock	5	8

- dry soil, $y >$20kT

$$SV_{20} = \begin{cases} 354 \times 10^{0.506\cdot[\exp(2.6\cdot S_2+0.486\cdot S_2^2)-1]+2\cdot S_2/9}, \\ \quad -3 \leqslant S_2 \leqslant 0 \\ 354 \cdot \exp\{[1-\exp(-3.967 \cdot S_2^{1.139})] \cdot [4.283 - 0.0515 \cdot (5-S_2)^{2.068}]\}, \\ \quad 0 \leqslant S_2 \leqslant 5 \end{cases} \tag{183}$$

- deeply buried for all material types:

$$SV = \exp(P + Q \cdot S_2 + R \cdot S_2^2) - S, \quad 5 \leqslant S_2 \leqslant 40 \tag{184}$$

where coefficients P, Q, R, S are tabulated below:

material type	no.	P	Q	R
dry soil	1	9.7	0.103	-0.00143
wet soil	2	12.54	0.029	-0.00078
dry soft rock	3	9.34	0.131	-0.00231
wet soft rock	4	10.45	0.089	-0.00134
hard rock	5	8.72	0.1634	-1/370

$$S = \begin{cases} 0, & \text{all materials but wet soil} \\ 503^2 \cdot \exp(-\dfrac{S_2}{30}), & \text{wet soil} \end{cases} \tag{185}$$

then:

- if $Y > 20$:

$$V = SV \cdot Y^{3\cdot\alpha} \tag{186}$$

– otherwise:

$$V = SV_{20} \cdot (\frac{SV_1}{SV_{20}})^g \cdot Y^\alpha \tag{187}$$

where SV_1 and SV_{20} are scaled volumes computed at 1 and 20 kT, i.e. $SV < 1 >$ and $SV < 20 >$.

Compute a volume for each layer separately, using the full yield, the relevant cratering efficiency, and the single-layer equations above: denoting these by V_{M1}, V_{M2}, V_{M3} if needed. Then, compute an average volume from these by the procedure described below:

$$2 \text{ layers:} V = \widehat{V_A} < V_{M1}, V_{M2}, T_1 > \tag{188}$$

$$3 \text{ layers:} V = \widehat{V_A} < V_{M1}, \widehat{V_A} < V_{M2}, V_{M3}, T_2 >, T_1 > \tag{189}$$

$\widehat{V_A} < V_U.V_L, T >$ is an approximation to $V_A < V_U, V_L, T >$ that satisfies the equation:

$$V_A = (V_L - V_U) \cdot \exp(-5.4 \cdot \frac{T}{V_A^{1/3}}) + V_U \tag{190}$$

where V_A is the average volume, the V_U the upper layer volume, V_L the lower layer volume, T the layer thickness. $\widehat{V_A}$ is computed iteratively by the procedure:

$$V_0 = \sqrt{V_U \cdot V_L} \tag{191}$$

$$V_{i+1} = (V_L - V_U) \cdot \exp(-5.4 \cdot \frac{T}{V_i^{1/3}}) + V_U \tag{192}$$

the apparent crater volume is equal to the fifth term in the series:

$$\widehat{V_A} = V_5 \tag{193}$$

Let $V = \widehat{V_A}$, the apparent crater radius, CR, and depth, CD are given by:

$$CR = 1.2 \cdot V^{1/3} \tag{194}$$

$$CD = 0.5 \cdot V^{1/3} \tag{195}$$

and the minimum ground range for debris calculation is then 1.8 times the apparent crater radius, CR. The ejecta thickness is given by the expression:

$$EJ = k \cdot V^{1.62} \cdot GR^{-3.86} \tag{196}$$

where

$$k = \begin{cases} 0.9, & \text{for dry and wet soil materials} \\ 1.17, & \text{for all rock materialss} \end{cases} \tag{197}$$

7 Fallout

This program uses a simplified version of the SIDAC/WSEG fallout model to perform the following calculations:

- The one-hour dose rate, the maximum biological dose and the time of arrival can be found as functions of weapon yield, height of burst, fission fraction, effective fallout wind speed, crosswind shear, distance downwind, and distance crosswind. The SIDAC model actually calculates the exposure (roentgen) and the exposure rate (roentgen per hour). In tissue, an exposure of 1 roentgen causes a dose of 0.96 rads, so close to 1 that the distinction between exposure (roentgen) and dose (rad) can be ignored when compared with other uncertainties of the model.
- Given a measurement of dose rate and the time at which it was taken, the program will find the one-hour dose rate. One hour is just a convenient and commonly-used reference time. The calculation assumes a time to the (-1.2) power dependence for dose rate.
- From a one-hour dose rate and a time of interest, the dose rate at that time can be calculated.
- The one-hour dose rate can be used to find the total dose if the time of entry and the duration of exposure are also given. The total dose is an integration of the dose-rate scaling law. Note that this is different from the maximum biological dose, which takes account of biological recovery that can occur over the course of an extended exposure.

The SIDAC fallout model calculates dose and dose rate at 3 feet above an infinite smooth plane. No shelter (shielding) factors have been applied, not even the 0.7 factor that is customarily used for the shielding provided by small surface irregularities on a real flat earth surface that is also called "smooth."

The basic fallout parameter is the hypothetical one-hour dose rate; it is the dose rate that would exist one hour after the detonation time if all the debris were deposited at that time. There is no implication that one-hour dose rate could actually be measured at a given location (the fallout may not even arrive by that time).

The effective fallout wind is a fall-time-weighted average wind (representative of the atmosphere through which the radioactive particles traverse), a function of the original height of the cloud. Crosswind shear obtained from the crosswind difference of effective winds for altitudes slightly above and below the cloud center.

The fundamental parameter used in determination of fallout fatalities and casualties is the maximum biological dose (MBD). The maximum biological dose allows for biological repair of radiation damage, 90% of the damage being assumed subject to repair and 10% not; the recovery rate is assumed to be 0.1% per hour. No shielding is assumed (e.g. terrain). MBD is calculated here by a method that is faster and more accurate than either of the two methods discussed in the source document.

ACCURACY:

The fits used in one-hour dose rate calculation, are in most cases identical to those mentioned in the source document. The major exception is the maximum

biological dose fit which was improved so that it would be in closer agreement with the theoretical function. The new MBD fit differs only ±5% on the average from theoretical values, with a worst case of 16% occurring for debris arrival times near the upper limit of 550 hours.

No accuracy claim is made for the SIDAC fallout model in the source document, but the reference report for a previous version of SIDAC (see the R. Mason report listed under REFERENCES) does discuss the accuracy of the older SIDAC model, and many of the conclusions are still relevant to the latest version.

A detailed comparison of the fallout model in SIDAC (sometimes called the Weapon Systems Evaluation Group or WSEG model) with two other models can be found in a report by H. Norment listed under REFERENCES. Again, the analysis was done using an older version of SIDAC, but many of the conclusions are still valid.

SOURCE OF DATA

- Mason, Ralph B. et. al., Description of Mathematics for the Single Integrated Damage Analysis Capability (SIDAC), Command and Control Technical Center Technical Memorandum TM-15-80, 13 June 1980.

OTHER REFERENCES

- Mason, Ralph B., Single Integrated Damage Analysis Capability (SIDAC),Functional Description, National Military Command System Support Center, System Planning Manual SPM FD 7-73, 1 January 1973.
- Norment, Hillyer, Evaluation of Three Fallout Prediction Models: DELFIC, SEER and WSEG-10, Atmospheric Science Associates, 28 April 1978 (draft report).

7.1 Fallout models

This model is reproduced without issue. This result matches the original to the fourth significant digit.

- Input and Limits:
  - Y, yield, kT, $0.1 \leqslant Y \leqslant 25{,}000$
  - H, height of burst, m, $0 \leqslant H \leqslant 4{,}000$
  - DW, downwind ground range, m , $0 \leqslant DW \leqslant 10^6$
  - CW, crosswind ground range, m, $0 \leqslant CW \leqslant 40{,}000$
  - W, effective wind speed, kn, $1 \leqslant W \leqslant 40$
  - SY, crosswind shear, kn/kft, $0 \leqslant SY \leqslant 10$
  - FF, fission fraction, 1, $0 \leqslant FF \leqslant 1$
  - T, measurement time, hr, $0.1 \leqslant T \leqslant 5000$
  - TI, initial exposure time, hr, $0.1 \leqslant TI \leqslant 5000$
  - TEXP, exposure duration, hr, $0 \leqslant TEXP \leqslant 5000\text{-}TI$
- Outputs:
  - DH + 1, one-hour dose rate, roentgen/hr
  - DT, t-hour dose rate, roentgen/hr

  - T0, debris arrival time, hours
  - MBD, maximum biological dose, roentgen
  - FD, total fallout dose, roentgen

- Models:

$$\widehat{H} = \frac{H}{0.3048} \tag{198}$$

  - for $\widehat{H} = 0$:

$$AF = 1 \tag{199}$$

  - for $\widehat{H} > 0$[6]:

$$z = 0.01 \cdot \frac{\widehat{H}}{Y^{0.4}} \tag{202}$$

$$AF = \begin{cases} 0, & z > 1 \\ 0.5 \cdot (1-z)^2 \cdot (2+z) + 0.001 \cdot z & z \leqslant 1 \end{cases} \tag{203}$$

in all cases,

$$Y_m = \frac{Y}{1,000} \tag{204}$$

cloud radius in nautical miles:

$$\sigma_0 = \begin{cases} Y_m^{1/3} \cdot \exp\{0.56 - \frac{3.25}{4 + (\ln(Y_m) + 5.4)^2}\}, & Y \geqslant 1 \\ 0.1 \cdot Y^{0.2665}, & Y < 1 \end{cases} \tag{205}$$

cloud height (in kilofeet)

$$h_0 = \begin{cases} 44 + 6.1 \cdot \ln(Y_m) - 0.205 \cdot [\ln(Y_m) + 2.42] \cdot |\ln(Y_m) + 2.42|, & Y \geqslant 1 \\ 6 \cdot Y^{0.25}, & Y < 1 \end{cases} \tag{206}$$

cloud duration (hours),

$$T_i = 1.057 \cdot h_0 \cdot (0.2 - \frac{h_0}{1,440}) \cdot [1 - 0.5 \cdot \exp(-\frac{h_0^2}{625})] \tag{207}$$

cloud thickness (kilofeet),

$$\sigma_h = 0.18 \cdot h_0 \tag{208}$$

[6]The equation in the main body is what is actually implemented in WE.EXE. In the original documentation, this section starts with:

$$z = 0.01 \cdot \frac{H}{Y^{0.4}} \tag{200}$$

which use the height of burst in meter instead of feet to initialize the value of z. We assume this is a typo in the documentation.

This is corroborated by quoting the section 5-97 of the EM-1 manual, where an "adjustment factor" (which shortens to AF) is mentioned for "transition height" above $100 \cdot W^{0.35}$ to $180 \cdot W^{0.4}$ feet:

$$\text{Adjustment Factor} = \frac{(180 - \frac{h}{W^{0.4}})^2 \cdot (360 + \frac{h}{W^{0.4}})}{1.17 \times 10^7} \approx \frac{(1 - \frac{h}{W^{0.4}})^2 \cdot (2 + \frac{h}{W^{0.4}})}{2} \tag{201}$$

with h in feet and W in kiloton. Clearly this form roughly correspond to part of the definition for AF. This form would not be possible if z was indeed in meters.

effective particle distance (nautical miles),

$$L_0 = W \cdot T_i \tag{209}$$

change in fallout distribution:

$$\sigma_x = \sigma_0 \sqrt{\frac{L_0^2 + 8 \cdot \sigma_0^2}{L_0^2 + 2 \cdot \sigma_0^2}} \tag{210}$$

a modified form of L_0

$$L = \sqrt{L_0^2 + 2 \cdot \sigma_x^2} \tag{211}$$

the constant for symmetry

$$N = \frac{L_0^2 + \sigma_x^2}{L_0^2 + 0.5 \cdot \sigma_x^2} \tag{212}$$

downwind distance (nautical miles)

$$d = \frac{DW}{1,853} \tag{213}$$

crosswind distance (nautical miles)

$$c = \frac{CW}{1,853} \tag{214}$$

area reduction factors,

$$\alpha_1 = (1 + 0.001 \cdot h_0 \cdot \frac{W}{\sigma_0})^{-1} \tag{215}$$

$$\alpha_2 = \{1 + 0.001 \cdot h_0 \cdot \frac{W}{\sigma_0} \cdot [1 - \Phi(2 \cdot \frac{d}{W})]\}^{-1} \tag{216}$$

where $\Phi(u)$ is the cumulative total distribution function, is approximated by the expression:

$$\Phi(u) = [1 + \exp(-1.5976 \cdot u - 0.0706 \cdot u^3)]^{-1} \tag{217}$$

the crosswind spread parameter:

$$\sigma_y = \sqrt{\sigma_0^2 \cdot R + 2 \cdot (P \cdot \sigma_x)^2 + (P \cdot Q \cdot L_0)^2} \tag{218}$$

where:

$$P = \frac{SY \cdot T_i \cdot \sigma_h}{L} \tag{219}$$

$$Q = \frac{|d + 2 \cdot \sigma_x|}{L} \tag{220}$$

$$R = \min(4, 1 + 8 \cdot Q) \tag{221}$$

the crosswind transport function,

$$F_1 = \frac{\exp[\frac{-(\frac{c}{\alpha_2 \sigma_y})^2}{2}]}{\sigma_y \cdot \sqrt{2\pi}} \tag{222}$$

the downwind transport function,

$$F_2 = \Phi(\frac{L_0 \cdot d}{L \cdot \alpha_1 \cdot \sigma_x}) \tag{223}$$

the deposition function,

$$F_3 = \frac{\exp(-|\frac{d}{L}|^N)}{L \cdot \Gamma(1 + \frac{1}{N})} \tag{224}$$

the gamma function can be approximated by the expression:

$$\Gamma(u) = 0.994 - 0.446 \cdot (u - 1) + 0.455 \cdot (u - 1)^2, \quad 1 \leqslant u \leqslant 2 \tag{225}$$

$$F = F_1 \cdot F_2 \cdot F_3 \tag{226}$$

the one-hour dose rate,

$$DH + 1 = 1,510 \cdot Y \cdot FF \cdot AF \cdot F \tag{227}$$

the debris arrival time,

$$T_0 = \sqrt{0.25 + \frac{(L_0 \cdot Q \cdot T_i)^2 + 2 \cdot \sigma_x^2}{L_0^2 + 0.5 \cdot \sigma_x^2}} \tag{228}$$

the maximum biological dose can be found using the equations:

$$z_0 = \ln(T_0) \tag{229}$$

$$MBD = (DH + 1) \cdot (2.737 - 0.7809 \cdot z_0 + 2 \cdot \frac{z_0^2}{29} - \frac{z_0^3}{617}) \tag{230}$$

the t-hour dose rate

$$DT = (DH + 1) \cdot T^{-1.2} \tag{231}$$

the fallout total dose:

$$FD = 5 \cdot (DH + 1) \cdot [TI^{-0.2} - (TI + TEXP)^{-0.2}] \tag{232}$$

A Thermal Fluence Required for Burn Damage

The required thermal fluence to cause a certain degree of burn damage for low altitude air burst is dependent on the time frame of the energy release, which tends to be longer for higher yield weapons. The Effects of Nuclear Weapon suggested a convenient linear relationship (on a log-linear plot) as following:

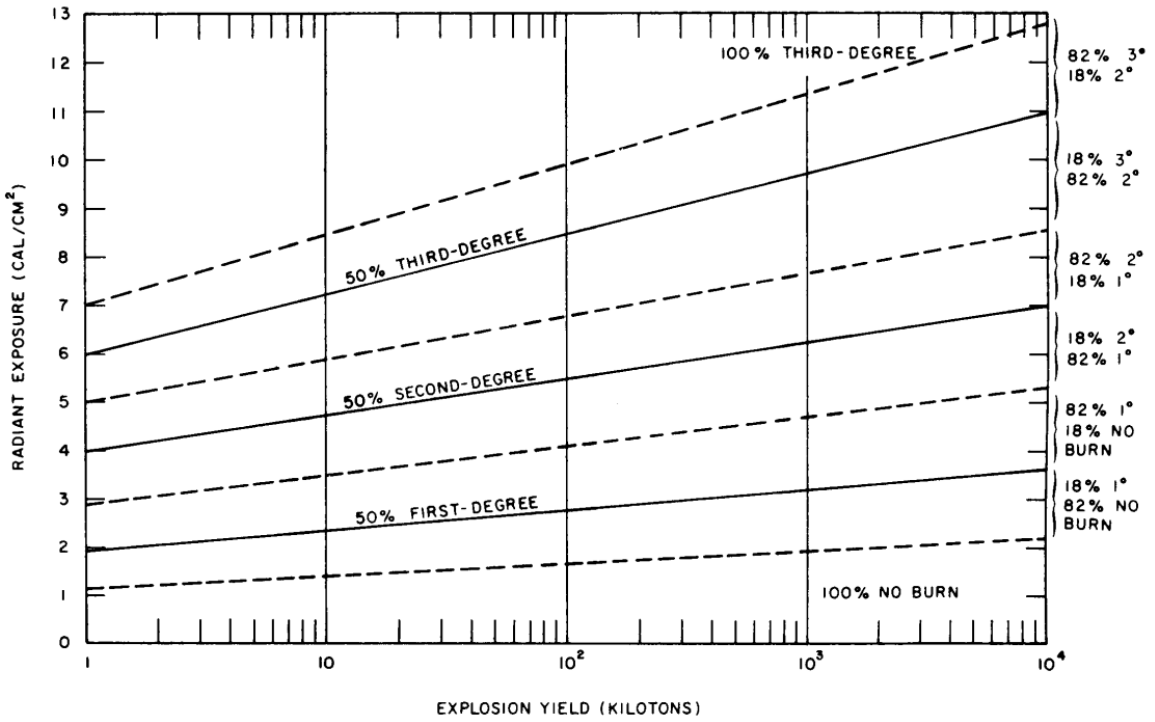

Figure 12.65. Skin burn probabilities for an average unshielded population taking no evasive action as a function of explosion yield and radiant exposure.

Figure 3: Effects of Nuclear Weapons (1977), Glasstone, S., Dolan, Philip J., section 12, figure 65, page 565.

From top to bottom, the various burn criteria have been fitted to be:

$$\mathrm{Q}<\mathrm{cal/cm^2}> = \begin{cases} 1.45 \cdot \log_{10}(\mathrm{Y}) + 7 \\ 1.25 \cdot \log_{10}(\mathrm{Y}) + 6 \\ 0.88 \cdot \log_{10}(\mathrm{Y}) + 5 \\ 0.75 \cdot \log_{10}(\mathrm{Y}) + 4 \\ 0.60 \cdot \log_{10}(\mathrm{Y}) + 2.85 \\ 0.41 \cdot \log_{10}(\mathrm{Y}) + 2 \\ 0.26 \cdot \log_{10}(\mathrm{Y}) + 1.1 \end{cases} \tag{233}$$

The underlying distribution for the probability of burns is a normal distribution with a mean of "50% value" in the above table, with the dotted levels being 1.17741(002) standard deviations from the expectation, i.e. $\Phi(-1.17741) \approx 11.95\%$, $\Phi(1.17741) \approx 88.05\%$ and $\phi(\pm 1.17741) \approx 0.5$. For best fit, use piecewise probability with standard deviation calculated for that branch.

B Deep Space Nuclear Detonation

Prompt radiation from nuclear detonation in free space is of interest.

C Prior Work: Analytic Approximation for Peak Overpressure Versus Burst Height and Ground Range Over an Ideal Surface

The work *Analytical Approximation for Peak Overpressure Versus Burst Height and Ground Range Over an Ideal Surface* by Stephen J. Speicher and Harold L. Brode as referenced in the main text is reproduced here in part:

One analytic approximation to the revised EM-1 HOB peak overpressure curves is reported in Chap. 7. (see Appendix D) The procedure uses an interpolation scheme between similarities in the HOB curves; the curves are illustrated in Figs. 1 through 3 below.

Another procedure was reported at an Airblast Working Group meeting at DNA on 12 December 1979. It did not provide as good a fit to the new EM-1 curves, but was somewhat simpler and more direct. Subsequent refinement of the earlier form has resulted in a better fit. It is suggested that this modified procedure be used in calculations of peak overpressure, since it is simpler and more accurate. We intend to use it in our analytic approximations to pressure-time histories, now being derived.

To proceed, given x, the scaled ground range, and y, the scaled height of burst, an overpressure is calculated as follows:[7] [8]

The peak overpressure $\Delta P < r, z >$ in kPa and km/kT$^{1/3}$ is then

$$r = \sqrt{x^2 + y^2} \tag{234}$$

$$z = y/x \tag{235}$$

and

$$\Delta P < r, z >= \beta \cdot [\frac{10.47}{(\alpha \cdot r)^{a<z>}} + \frac{b < z >}{(\alpha \cdot r)^{c<z>}} + \frac{d < z > \cdot e < z >}{1 + f < z > \cdot (\alpha \cdot r)^{g<z>}} + h < z, r, y >] \tag{236}$$

where

$$h < z, r, y >= \frac{-64.67 \cdot z^5 - 0.2905}{1 + 441.5 \cdot z^5} - \frac{1.389 \cdot z}{1 + 49.03 \cdot z^5} + \frac{8.808 \cdot z^{1.5}}{1 + 154.5 \cdot z^{3.5}} + \frac{0.0014 \cdot (\alpha \cdot r)^2}{(1 + 2 \cdot y) \cdot [1 - 0.158 \cdot (\alpha \cdot r) + 0.0486 \cdot (\alpha \cdot r)^{1.5} + 0.00128 \cdot (\alpha \cdot r)^2]} \tag{237}$$

and where

$$a < z > = 1.22 - \frac{3.908 \cdot z^2}{1 + 810.2 \cdot z^5} \tag{238}$$

$$b < z > = 2.321 + \frac{6.195 \cdot z^{18}}{1 + 1.113 \cdot z^{18}} - \frac{0.03831 \cdot z^{17}}{1 + 0.02415 \cdot z^{17}} + \frac{0.6692}{1 + 4,164 \cdot z^8} \tag{239}$$

[7] The range of pressures for which the procedure is intended is from 1 to 10,000 psi (7 kPa to 70 MPa); all distances are in scaled kilofeet (kft/kT$^{1/3}$) or kilometers (km/kT$^{1/3}$).

[8] To avoid the singularity in z as x $\rightarrow$ 0, it is suggested that a small number limit be placed on x, and the magnitude of z be limited so as not to overflow when z is raised to the 18th power. These values are machine-dependent.

$$c < z > = 4.153 - \frac{1.149 \cdot z^{18}}{1 + 1.641 \cdot z^{18}} - \frac{1.1}{1 + 2.771 \cdot z^{2.5}} \tag{240}$$

$$d < z > = -4.166 + \frac{25.76 \cdot z^{1.75}}{1 + 1.382 \cdot z^{18}} - \frac{8.257 \cdot z}{1 + 3.219 \cdot z} \tag{241}$$

$$e < z > = 1 - \frac{0.004642 \cdot z^{18}}{1 + 0.003886 \cdot z^{18}} \tag{242}$$

$$f < z > = 0.6096 + \frac{2.879 \cdot z^{9.25}}{1 + 2.359 \cdot z^{14.5}} - \frac{17.15 \cdot z^2}{1 + 71.66 \cdot z^3} \tag{243}$$

$$g < z > = 1.83 + \frac{5.361 \cdot z^2}{1 + 0.3139 \cdot z^6} \tag{244}$$

with

$$\alpha = 1/0.3048 \qquad \texttt{kft/km} \tag{245}$$

$$\beta = \frac{100}{14.504} \qquad \texttt{kPa/psi} \tag{246}$$

(US customary unit formulations, test cases, and figures elided for brevity) ......Since the disparity is much less than the accuracy of the original curves, and very much less than the scatter in supporting data, we suggest that the fit generated curves could be substituted without loss of validity. There would then be no difference between displayed curves and analytic approximations to confuse the novice user.

D Prior Work: Analytic Approximation for Dynamic Pressure Versus Time

The *Revised Procedure for The Analytic Approximation of Dynamic Pressure Versus Time* was referenced in the main text. It builds upon the prior work titled *Analytic Approximation for Dynamic Pressure Versus Time* by the same author, Stephen J. Speicher and Harold L.Brode, which is reproduced in part here.

The procedure reported here was contrived to satisfy a limited request: for dynamic pressure as a function of burst height for 5, 15, and 25 psi at scaled burst heights of 0, 200, and 700 ft, for 40 kT. The procedure, which may be extended to broader applications at a later date, is designed to use the approximations given in Brode [1970], but can readily be adapted to the new fit to peak overpressure, which corresponds to the recently recommended correction curves for EM-1. (The new fit was reported at the 31 March 1980 meeting (at RDA, Marina del Rey, California) of the DNA Airblast Working Group, and in PSR's progress report for December 1979 through February 1980 on Contract DNA001-80-C-0065.) The steps in the approximation are as follows:

- *Given*:
  - y, Height of burst (HOB), kft
  - x, Ground range, kft
  - W, Yield, kT
- *Step 1. Solve for* $t_a < r, W >$ *[free air burst]*:
  The free-air-burst time-of-arrival derived from Eq. (5) of Brode [1970]:

$$t_a = \frac{0.5429 \cdot m^3 - 21.185 \cdot r \cdot m^2 + 361.8 \cdot r^2 \cdot m + 2,383 \cdot r^3}{m^2 + 2.048 \cdot r \cdot m + 2.6872 \cdot r^2} \quad \text{millisecond} \tag{247}$$

  where:

$$m = W^{1/3} \tag{248}$$

$$r = \sqrt{x^2 + y^2} \tag{249}$$

- *Step 2. Solve for* $\Delta P_s < t_a, W >$ *[free-air burst]:*
  Next, the free-air-burst peak overpressure at this range, HOB and yield, using Eq. (13) of Brode [1970], with $t = t_a$. (For overpressures above 1000 psi, Brode's Eq. (13) has been modified to give faster decay from the peak; but the correction is irrelevant for the dynamic pressure application here, which uses only peak overpressure.) For peak overpressure, with $t = t_a$, Brode's Eq. (13) becomes:

$$\Delta P_s < t_a, W >= \frac{14,843 \cdot m}{0.0135 \cdot m + t_a} \cdot \left(\frac{m^2 + 0.6715 \cdot m \cdot t_a + 0.00481 \cdot t_a^2}{m^2 + 1.8836 \cdot m \cdot t_a + 0.02161 \cdot t_a^2}\right) \quad \text{psi} \tag{250}$$

  A simpler form appropriate for peak overpressure is:

$$\Delta P_s < t_a, W >= \frac{1.05 \times 10^6}{1 + 130 \cdot t^{1.14}} \quad \text{psi} \tag{251}$$

where $t = t_a/m$. This expression is reasonable from 2 psi to 1 million psi, and is accurate to within 10 percent in the range 2 to 10,000 psi.

(Figure of comparison was elided for brevity)

Both Eqs. (2) and (3) (249,250 in this document) represent the peak overpressure for a free-air burst as a function of arrival time (and yield). A surface burst is approximated by the same form, with $2 \cdot W$ in place of W ($2^{1/3} \cdot m$ in place of m).

- *Step 3. Solve for* $t_a < x, y, W >$ *[HOB]:*
  For bursts near but not on the ground surface, arrival time is approximated by Eq. (16) of Brode [1970]:

$$t_a < x, y, W >= \begin{cases} t_a < r, W > & \text{for } x \leqslant y \\ t_a < r, W > \cdot y/x + t_a < r, 2 \cdot W > \cdot (1 - y)/x & \text{for } x \geqslant y \end{cases} \quad (252)$$

[9]

- *Step 4. Solve for* $\Delta P_s < t_a, x, y, W >$ *[HOB]:*
  Peak overpressure as approximated by Eq. (20) of Brode [1970] is:

$$\Delta P_s < P, z >= H < P, z > \cdot [1 + \frac{E < P >}{1 + 0.4/z^4}]$$

$$\times [a \cdot \Delta P_s < t_a, W > + (1 - a) \cdot \Delta P_s < t_a, 2W >] \quad (254)$$

where $\Delta P_s < t_a, W >$ and $\Delta P_s < t, 2W >$ are defined by Eq. (2) or (3) (249,250 in this document) above:

$$z = \frac{y}{x \cdot t_a} \quad (255)$$

$$P = \frac{1.58 \cdot W}{r^3} + \frac{5.3 \cdot \sqrt{W/r}}{r} + 0.0215 \quad \text{(Eq. (1) of Brode [1970])} \quad (256)$$

$$H < P, z > = 1 + A + \frac{B \cdot P^{3/2}}{C + P^3} + \frac{F \cdot P}{I + P^2} \quad (257)$$

$$A = \frac{0.743 \cdot (1.136 - z) \cdot z^2}{1.544 + z^6} - \frac{0.0257 \cdot z^6}{0.004435 + z^{12}} \quad (258)$$

$$B = \frac{z \cdot (20.42 + 35.5 \cdot z)}{3.57 + z^2} + \frac{2,500 \cdot z^4}{29.3 + z^{14}} \quad (259)$$

$$C = [1 + \frac{z \cdot (2.23 \cdot z - 0.225)}{0.148 + z^2} + \frac{28.4 \cdot z^7}{0.905 + z^7}]^3 \quad (260)$$

$$E < P > = 1 + \frac{0.002655 \cdot P}{1 + 0.0001728 \cdot P + 1.921 \times 10^{-9} \cdot P^2} \quad (261)$$

[9] This is likely a typographical mistake: analysis of the limiting case of $x = y$ suggest one possible correction:

$$t_a < r, W > \cdot y/x + t_a < r, 2 \cdot W > \cdot (1 - y/x) \quad \text{for } x \geqslant y \quad (253)$$

$$+\frac{0.004218+0.04824\cdot \mathrm{P}+6.856\times 10^{-6}\cdot \mathrm{P}^2}{1+0.008\cdot \mathrm{P}+3.844\times 10^{-6}\cdot \mathrm{P}^2} \tag{262}$$

$$\mathrm{F}=\frac{2.07\cdot z^2}{0.00125+0.0146\cdot z^2+z^8}+\frac{221.25\cdot z^8}{1+z^{20}} \tag{263}$$

$$\mathrm{I}=40,000-\frac{17,650\cdot z^2}{0.235+z^6} \tag{264}$$

and finally:

$$\mathrm{a}=\frac{z^2\cdot(1+2\cdot z^4)}{1+2\cdot z^6} \tag{265}$$

Any other definition of the peak-overpressure/HOB/range relationship can, of course, be used at this step. One example is the new fit for the revised EM-1 curves, which take advantage of the similarities in the family of HOB curves from 1.0 to 10,000 psi. The behavior along the x-axis (zero HOB) is that of a surface burst, for which overpressure can be expressed as a simple function of ground range:

$$\mathrm{PD}\approx\frac{6.5}{\mathrm{x}^{4/3}}+\frac{4}{\mathrm{x}^3}\quad \mathrm{psi} \tag{266}$$

Along the vertical axis:

$$\mathrm{PK}\approx\frac{11}{\mathrm{y}^{1.3}}+\frac{6}{\mathrm{y}^{3.5}}\quad \mathrm{psi} \tag{267}$$

where x and y are in kft.

Along a curve through the maximum horizontal range for each isobar (y = RA), pressure is expressed by:

$$\mathrm{PE}\approx\frac{1.8}{\mathrm{x}^{3.4}}+\frac{4.4\times 10^5\cdot \mathrm{x}^9}{1+2.8\times 10^4\cdot \mathrm{x}^{10}}-\frac{5\cdot \mathrm{RA}^{2.3}}{1+\mathrm{RA}^{4.8}}-0.22\cdot \mathrm{RA} \tag{268}$$

where the curve

$$\mathrm{y}=\mathrm{RA}=1\times 10^{-4}\cdot \mathrm{x}^2+0.7\cdot\sqrt{\mathrm{x}}-\frac{0.12\cdot \mathrm{x}^{0.02}}{1+297\cdot \mathrm{x}^{4.0}}-0.23 \tag{269}$$

Along a curve through the relative minimum above the knees (y = RM), pressure is approximated as:

$$\mathrm{PJ}\approx\frac{14.35}{\mathrm{RI}^{1.45}}+0.056+\frac{4}{\mathrm{RI}^{3.71}}-\frac{0.171}{\mathrm{RI}^{4.716}} \tag{270}$$

where $\mathrm{RI}=\sqrt{\mathrm{RF}^2+\mathrm{y}^2}$, with:

$$\mathrm{RF}\approx 4.1\cdot \mathrm{y}^{0.76}-2.3\cdot \mathrm{y}^{0.31}+\frac{10.3\cdot \mathrm{y}^{1.8}}{1+231\cdot \mathrm{y}^{2.1}}-\frac{2.29\cdot \mathrm{y}^{1.3}}{1+\mathrm{y}^{2.2}}+0.56 \tag{271}$$

Interpolating between the pressures along the four curves $\mathrm{y}=0, \mathrm{x}=0, \mathrm{y}=\mathrm{RA}<\mathrm{x}>$ and $\mathrm{x}=\mathrm{RF}<\mathrm{y}>$ defines the peak overpressure for any height of burst (y) and range (x).

The interpolation is not linear and differs in each region. In region I, between $\mathrm{y}=0$ and $\mathrm{y}=\mathrm{RA}$:

$$\Delta \mathrm{P_s}\approx(1-\mathrm{FC})\cdot \mathrm{PD}+\mathrm{FC}\cdot \mathrm{PE} \tag{272}$$

where:

$$FC \approx FB \cdot \frac{0.433 + 1.011 \cdot FB}{1 + 0.444 \cdot FB^5} \tag{273}$$

and:

$$FB = \frac{y}{RA} \tag{274}$$

In region II, between $y = RA < x >$ and $x = RF < y >$:

$$\Delta P_s \approx FO \cdot PL + (1 - FP) \cdot FC \cdot PE \tag{275}$$

where:

$$FO \approx 0.77 \cdot FN^{2.74} + 0.23 \cdot FN^{0.70} \tag{276}$$

$$FN \approx \frac{y \cdot (y - RA)}{RM \cdot (RM - RA)} \tag{277}$$

$$FP \approx FO^{[1+0.00594\cdot(x^2+y^2)^{1.28}]} \tag{278}$$

$$PL \approx (1 - FH) \cdot PK + FH \cdot PJ \tag{279}$$

$$FH \approx 0.093 \cdot FG^{1.03} + \frac{7.7 \cdot FG^{2.51}}{1 + 7.49 \cdot FG^{2.15}} \tag{280}$$

$$FG = \frac{x}{RF} \tag{281}$$

and:

$$RM \approx 0.0036 - \frac{0.092 \cdot x^{-0.39}}{1 + 31 \cdot x^{3.11}} + \frac{0.69 \cdot x^{0.46}}{1 - 0.2 \cdot x^{0.47}} + \frac{0.006}{x^{1.11}} \tag{282}$$

In region III:

$$\Delta P_s \approx PL \tag{283}$$

- *Step 5. Solve for* $Q_s < \Delta P_s >$ *[HOB]* Peak dynamic pressure in an adiabatic shock is directly related to peak overpressure by the expression:

$$Q_s = \frac{\Delta P_s^2}{2 \cdot \gamma \cdot P_0 + (\gamma - 1) \cdot P_s} \tag{284}$$

[10] where P_0 is the ambient air (preshock) pressure and γ is the effective specific heat ratio for air. For overpressures less than 300 psi, γ may be approximated as 1.4. For all overpressures at sea level ($P_0 \approx 14.7$ psi or 10^5 Pa), $1.16 < \gamma < 1.67$ [Brode, 1968].

For the revised peak overpressure fit [Eqs. (6) through (14)], (265 to 281 in this document) , peak values do not in all cases correspond to shock front values: in part of the Mach reflection region, the second peak exceeds the shock value, so that the Hugoniot (shock) expression for dynamic pressure is

[10] Comparing against the expression for dynamic pressure in S. Glasstone and P. J. Dolan, *Effects of Nuclear Weapons*, 1977 equation (3.55.1), this can be best clarified to:

$$Q_s = \frac{\Delta P_s^2}{2 \cdot \gamma \cdot P_0 + (\gamma - 1) \cdot \Delta P_s} \tag{285}$$

not rigorously valid in that region. However, since both peak overpressure and dynamic pressure increase in the double Mach region, we assume the same relation applies.

In the regular reflection region, effective dynamic pressure does not equal total dynamic pressure, since at the surface the flow is constrained to horizonral velocities only. An approximate correction for that effect is to express horizontal dynamic pressure as:

$$Q_H < x, y >= Q_s < r_s > \cdot \frac{x}{y} \quad \text{for x<y} \tag{286}$$

In the Mach reflection region, the flow has presumably been turned parallel to the surface, and the horizontal component is the total dynamic pressure:

$$Q_H < x, y >= Q_s < r_s > \quad \text{for } x \geqslant y \tag{287}$$

Although the transition between regular and Mach reflection does not occur exactly at $x = y$, the approximation brings the horizontal dynamic pressure to zero at the point on the surface directly beneath the burst (x = 0), and allows full dynamic forces as the shock passes into the Mach region.

- *Solve for Q<t>* The following approximation for dynamic pressure as a function of HOB, range, time, and yield is based on the observation that dynamic pressure behind the shock front at any time is a rapidly decreasing function of distance behind the front. A reasonable approximation is:

$$Q < r >= Q < r_s > \cdot (r_0/r_s)^9 \tag{288}$$

where $r_0 = \sqrt{x_0^2 + y^2}$, with x_0 the original ground range of interest; and $r_s = \sqrt{x^2 + y^2}$, with x the subsequent shock position ground range. Thus, if t_0 represents the shock arrival time at the position of interest (x_0, y) and t represents the shock arrival time as further position (x, y),

$$Q < t >= Q_H < x, y > \cdot (r_0/r)^9 \tag{289}$$

and x, r, t are related by $r = \sqrt{x^2 + y^2}$, $t = t_a < r, W >$ [Eq. (1)]. (Equation 246 in this document)

The ninth-power decay is only an approximation to the dynamic pressure behavior behind the shock front at low pressures (5 to 30 psi). The best fit power in this range varies between 8.8 and 10.2 [Brode, 1966, Fig. 37 and 38]; (figure elided for brevity)

(explanation for tables attached elided for brevity) ..... The impulse is the partial integral

$$I < t >= \int_{t_0}^{t} Q < t > dt \tag{290}$$

(further discussion of tables attached elided for brevity)

The approximation outlined above makes use of the rapid decay of dynamic pressure behind the shock front from a free-air burst, but even that decay may not be rapid enough in the early Mach reflection region. Preliminary study of the results of the 200-ft-HOB HULL calculation [McNamara, Jordano, and Lewis, 1977] suggests that the dynamic impulse in the Mach region where

the second peak is the larger is not as strongly influenced by HOB as are peak overpressure and corresponding peak dynamic pressure. This is not likely to be the case unless the early dynamic pressure fades more rapidly behind the shock than does the free-air dynamic pressure. Thus, dynamic pressure impulse HOB curves should have less pronounced knees.

This conjecture is a preliminary one, based solely on unverified observations from a numerical calculation; a physical explanation does not yet exist. However, if true, the fit suggested here would need further modification in the Mach reflection region.

References:

- Brode, Harold L., *Height of Burst Effects at High Overpressures*, The Rand Corporation, RM-6301-DASA, 1970 (DASA Report 2506).
- "Review of Nuclear Weapons Effects," *Annu. Rev. Nucl. Sci.*, 1968.
- -----, *Theoretical Description of the Blast and Fireball for a Sea Level Kiloton Explosion*, The Rand Corporation, RM-2246-PR, 1966.
- -----, *Theoretical Description of the Blast and Fireball for a Sea Level Megaton Explosion*, The Rand Corporation, RM-2248, 1959.
- McNamara, W., R. J. Jordana (GE Tempo), and P. S. Lewis (McDonnell Douglas Astronautics), *Airblast from a One Kiloton Nuclear Burst at 60 m over an Ideal Surface*, Contract Report 353, November 1977.
- Needham, Charles E., Martin L. Havens, and Carolyn S. Knauth, *Nuclear Blast Standard (1 KT)*, Air Force Weapons Laboratory, Report AFWL-TR-73-55 (rev), April 1975.

E Prior Work: Revised Procedure for Analytic Approximation of Dynamic Pressure Versus Time

The *Revised Procedure for The Analytic Approximation of Dynamic Pressure Versus Time* by Stephen J. Speicher and Harold L. Brode was referenced in the main text, and reproduced in part here.

The procedure for calculating height-of-burst dynamic pressure given in Chap. 6 was contrived to satisfy a limited request in a narrow pressure range. The procedure is here extended to the full range of pressure interests, using a new analytic fit for the duration of the dynamic pressure positive phase.

The original form used was [Chap. 6, Eq. (17)] (see appendix D equation 287)

$$Q < r >= Q < r_s > \cdot(\frac{r_0}{r_s})^9 \tag{291}$$

where $r_0 = \sqrt{x_0^2 + y^2}$, with x_0 the original ground range of interest; and $r_s = \sqrt{x^2 + y^2}$, with x the subsequent shock position ground range. Thus, if t_0 represents the shock arrival time at the position of interest $(x0, y)$, and t represents the shock arrival time at further positions (x, y) [Chap. 6, Eq. (18)] (see appendix D equation 288) , then

$$Q < t >= Q_H < x, y > \cdot(\frac{r_0}{r})^9 \tag{292}$$

and x, r, and t are related by $r = \sqrt{x^2 + y^2}$, $t = t_a < r, W >$ [Chap.6, Eq. (4)] (see equation 251).

The extended procedure now takes the form

$$Q < t >= Q_H < x, y > \cdot(\frac{r_0}{r})^n \cdot [1 - (\frac{t - t_0}{D_u^+})^2] \tag{293}$$

where n is a variable power such that:

$$n < r, m >= 0.7917 + 11.04 \cdot \frac{r}{m} + \frac{14.37 + 6.291 \cdot \frac{r}{m}}{1 + 28.41 \cdot (\frac{r}{m})^3} \tag{294}$$

and the positive (outward) wind duration is approximated as

$$D_u^+ < r_0, m' >= m' \cdot [\frac{0.2455 - 0.0115 \cdot \frac{r_0}{m'}}{1 + 61.43 \cdot (\frac{r_0}{m'})^6} + \frac{2.177 \cdot (\frac{r_0}{m'})^3}{1 + 0.7567 \cdot (\frac{r_0}{m'})^2 + 6.147 \cdot (\frac{r_0}{m'})^3} - 0.05546] \tag{295}$$

where r, r_0 , t, and t_0 are defined above, and

$$m = W^{1/3}, \quad m' = (2 \cdot W)^{1/3} \tag{296}$$

The units for these quantities are x, y, r, r_0 (kft); W, m, m' (kT and $kT^{1/3}$); D_u^+ (sec).

The virtue of the new procedure is that the total dynamic impulse can now be calculated to the cutoff of the dynamic positive phase, and the variable power n can now track the decay rate changes in different pressure regions. More important, the correct total dynamic impulse is simulated.

.....The positive phase duration D_u^+ is a very close approximation (within 2 percent) to data presented in Brode [1959].....this approximation with the AFWL

data reveals considerable discrepancy This may be due to differences in interpretation of the start of the negative phase, which would change both the duration (sec) and effective range at which the velocity first reverses.....

(graphs & comparisons elided for brevity)

It is clear that the new procedure tends to reduce the total impulse, substantially so at the lower overpressure. This occurs because the variable power in Eq. (1) (equation 292) tracks a faster decay rate than the constant power used in Eq. (17) of Chap. 6 (equation 287 of appendix D). The new EM-1 approximations further reduce the total impulse.

References:

- Brode, Harold L., *Height of Burst Effects at High Overpressure* The Rand Corporation, RM-6301-DASA, 1970 (DASA report 2506).
- -----, *Theoretical Description of the Blast and Fireball for a Sea Level Megaton Explosion*, The Rand Corporation, RM-2248, 1959.
- Needham, Charles E., Martin L. Havens, and Carolyn S. Knauth, *Nuclear Blast Standard (1 kT)*, Air Force Weapons Laboratory, Report. AFWL-TR-73-55 (rev.), April 1975.

F Prior Work: New Analytic Fit for Revised EM-1 Curves

Although not referenced in the body, this work introduced an improved fit using the methods first outlined in *Analytic Approximation for Dynamic Pressure Versus Time*. This is reproduced here due to the resemblance of the methods described to those present in the BLAST program.

The new fit takes advantage of the similarities evident in the family of HOB curves from 1.0 to 10,000 psi. The behavior along the x-axis (zero HOB) is that of a surface burst, for which overpressure can be expressed as a simple function of ground range:

$$\mathsf{PD} = \frac{6.48}{\mathsf{x}^{1.2518}} + \frac{3.9727}{\mathsf{x}^{2.924}} \quad \text{psi} \tag{297}$$

Along the vertical axis (zero ground range), the behavior is approximated by

$$\mathsf{PK} = \frac{11.049}{\mathsf{y}^{1.3069}} + \frac{6.0481}{\mathsf{y}^{3.4793}} \quad \text{psi} \tag{298}$$

in which x snf y are in $\text{kft/kT}^{1/3}$.

Along a curve through the maximum horizontal range for each isobar ($\mathsf{y} = \mathsf{RA}$), the pressure is expressed by

$$\mathsf{PE} = \frac{1.7934}{\mathsf{x}^{3.4227}} + \frac{441,830 \cdot \mathsf{x}^{8.7266}}{1 + 28,242 \cdot \mathsf{x}^{9.661}} - \frac{5 \cdot \mathsf{RA}^{2.2643}}{1 + 1.0453 \cdot \mathsf{RA}^{4.8336}} - 0.21915 \cdot \mathsf{RA} \tag{299}$$

where the curve

$$\mathsf{y} = \mathsf{RA} = 0.00009686 \cdot \mathsf{x}^{2.045} + 0.6857 \cdot \mathsf{x}^{0.4906} - \frac{0.1176 \cdot \mathsf{x}^{0.01869}}{1 + 296.5 \cdot \mathsf{x}^{3.962}} - 0.02255 \tag{300}$$

Along a curve through the relative minimum above the knees ($\mathsf{y} = \mathsf{RM}$ or $\mathsf{x} = \mathsf{RF}$), the pressure is approximated as

$$\mathsf{PJ} = \frac{14.35}{\mathsf{RI}^{1.45}} + 0.056 + \frac{4}{\mathsf{RI}^{3.71}} - \frac{0.171}{\mathsf{RI}^{4.716}} \tag{301}$$

in which $\mathsf{RI} = \sqrt{\mathsf{RF}^2 + \mathsf{y}^2}$, with

$$\mathsf{RF} = 4.106 \cdot \mathsf{y}^{0.7555} - 2.317 \cdot \mathsf{y}^{0.3074} + \frac{10.3 \cdot \mathsf{y}^{1.803}}{1 + 230.8 \cdot \mathsf{y}^{2.132}} - \frac{2.286 \cdot \mathsf{y}^{1.291}}{1 + 1.006 \cdot \mathsf{y}^{2.236}} + 0.5642 \tag{302}$$

Interpolating between the pressures along the four curves $\mathsf{y} = 0$, $\mathsf{x} = 0$, $\mathsf{y} = \mathsf{RA} < \mathsf{x} >$, and $\mathsf{x} = \mathsf{RF} < \mathsf{y} >$ defines peak overpressure for any height of burst (y) and range (x).

The interpolation is not linear and differs in each region. In region I, between $\mathsf{y} = 0$ and $\mathsf{y} = \mathsf{RA}$,

$$\Delta \mathsf{P_s} \approx (1 - \mathsf{FC}) \cdot \mathsf{PD} + \mathsf{FC} \cdot \mathsf{PE} \tag{303}$$

where

$$\mathsf{FC} = \frac{\mathsf{FB} \cdot (0.433 + 1.011 \cdot \mathsf{FB})}{1 + 0.444 \cdot \mathsf{FB}^5} \tag{304}$$

and

$$\mathsf{FB} = \frac{\mathsf{y}}{\mathsf{RA}} \tag{305}$$

In region II, between $\mathsf{y} = \mathsf{RA} < \mathsf{x} >$ and $\mathsf{x} = \mathsf{RF} < \mathsf{y} >$,

$$\Delta \mathsf{P_s} \approx \mathsf{FO} \cdot \mathsf{PL} + (1 - \mathsf{FP}) \cdot \mathsf{FC} \cdot \mathsf{PE} \tag{306}$$

where

$$FO = 0.7717 \cdot FN^{2.743} + 0.2283 \cdot FN^{0.7} \tag{307}$$

$$FN \approx \frac{y \cdot (y - RA)}{RM \cdot (RM - RA)} \tag{308}$$

$$FP = FO^{1+0.00594\cdot(\sqrt{x^2+y^2})^{2.565}} \tag{309}$$

$$PL \approx (1 - FH) \cdot PK + FH \cdot PJ \tag{310}$$

$$FH = 0.09284 \cdot FG^{1.0286} + \frac{7.696 \cdot FG^{2.513}}{1 + 7.4836 \cdot FG^{2.151}} \tag{311}$$

$$FG = \frac{x}{RF} \tag{312}$$

and

$$RM = \frac{-0.09175 \cdot x^{-0.3896}}{1 + 31.31 \cdot x^{3.106}} + 0.003582 + \frac{0.6907 \cdot x^{0.4597}}{1 - 0.2021 \cdot x^{0.4696}} + \frac{0.005963}{x^{1.106}} \tag{313}$$

In region III,

$$\Delta P_s \approx PL \tag{314}$$

This fit provides a continuous analytic approximation to the new (and improved) peak overpressure curves recommended for EM-1.